**Article:**
(2020) Broad and strong memory CD4+ and CD8+ T cells induced by SARS-CoV-2 in UK convalescent individuals following COVID-19. Nature immunology. 1336–1345. ISSN 1529-2916

https://doi.org/10.1038/s41590-020-0782-6

# Broad and strong memory CD4$^+$ and CD8$^+$ T cells induced by SARS-CoV-2 in UK convalescent COVID-19 patients

Yanchun Peng[1,2†], Alexander J. Mentzer[3,4,20†], Guihai Liu[2,4,5†], Xuan Yao[1,2,4†], Zixi Yin[1,2†], Danning Dong[2,4,6†], Wanwisa Dejnirattisai[4†], Timothy Rostron[7], Piyada Supasa[4], Chang Liu[2,4], César López-Camacho [3,4], Jose Slon-campos[4], Yuguang Zhao[4], David I. Stuart[2,3,4,17], Guido C. Paesen[3], Jonathan Grimes[3,4,17], Alfred A. Antson[8], Oliver W. Bayfield[8], Dorothy EDP. Hawkins[8], De-Sheng Ker[8], Beibei Wang[2,4], Lance Turtle[9,13], Krishanthi Subramaniam[13], Paul Thomson[13], Ping Zhang[4], Christina Dold[10], Jeremy Ratcliff[4], Peter Simmonds[4], Thushan de Silva[11], Paul Sopp[7], Dannielle Wellington[1,2], Ushani Rajapaksa[2,4] , Yi-Ling Chen[1], Mariolina Salio[1], Giorgio Napolitani[1], Wayne Paes[4], Persephone Borrow[4], Benedikt M. Kessler[2,4], Jeremy W. Fry[12], Nikolai F. Schwabe [12], Malcolm G Semple[13,14], J. Kenneth Baillie[15], Shona C. Moore[13], Peter JM Openshaw[16], M. Azim Ansari[4], Susanna Dunachie[4,20], Eleanor Barnes[4,20,21], John Frater [4,20], Georgina Kerr[4], Philip Goulder[4,20], Teresa Lockett[20], Robert Levin[18], Yonghong Zhang[2,5], Ronghua Jing[5], Ling-Pei Ho[1,2,4,21], Oxford Immunology Network Covid-19 Response T cell Consortium, ISARIC4C Investigators, Richard J. Cornall[1,4,20], Christopher P. Conlon[2,4,20], Paul Klenerman[4,20,21], Gavin R. Screaton[4,20,21], Juthathip Mongkolsapaya[2,4,19,21], Andrew McMichael[2,4], Julian C. Knight[2,3,4,20], Graham Ogg[1,2,20,21‡], Tao Dong [1,2,4‡*]

1. MRC Human Immunology Unit, MRC Weatherall Institute of Molecular Medicine, Radcliffe Department of Medicine, University of Oxford, Oxford, U.K.
2. Chinese Academy of Medical Science (CAMS) Oxford Institute (COI), University of Oxford, Oxford, U.K.
3. Wellcome Centre for Human Genetics, University of Oxford, Oxford, U.K.
4. Nuffield Department of Medicine, University of Oxford, Oxford, U.K.
5. Beijing You'an Hospital, Capital Medical University, Beijing, China

6. CAMS Key Laboratory of Tumor Immunology and Radiation Therapy, Xinjiang Tumor Hospital, Xinjiang Medical University, China.

7.Sequencing and Flow cytometry facility, Weatherall Institute of Molecular Medicine, University of Oxford, Oxford, UK

8. York Structural Biology Laboratory, Department of Chemistry, University of York, York, UK

9. Tropical and Infectious Disease Unit, Liverpool University Hospitals NHS Foundation Trust

10. Oxford Vaccine Group, Department of Paediatrics, University of Oxford, and NIHR Oxford Biomedical Research Centre, Centre for Clinical Vaccinology and Tropical Medicine, University of Oxford, UK

11. The Florey Institute for Host-Pathogen Interactions, Dept. of Infection, Immunity and Cardiovascular Disease, University of Sheffield, Sheffield, UK

12. ProImmune Limited, Oxford, UK

13. NIHR Health Protection Research Unit in Emerging and Zoonotic Infections, Institute of Infection, Veterinary & Ecological Sciences, University of Liverpool, Liverpool, UK

14. Respiratory Medicine, Institute in The Park, Alder Hey Children's Hospital, Liverpool, UK11. 15. Anaesthesia, Critical Care and Pain Medicine Division of Health Sciences, University of Edinburgh, Edinburgh, UK

16. National Heart and Lung Institute, Faculty of Medicine, Imperial College London, London, UK

17. Diamond Light Source, Didcot, UK.

18. Worthing Hospital, Worthing, UK

19. Dengue Hemorrhagic Fever Research Unit, Office for Research and Development, Faculty of Medicine, Siriraj Hospital, Mahidol University, Bangkok, Thailand

20. Oxford University Hospitals NHS Foundation Trust, Oxford

21. NIHR Oxford Biomedical Research Centre

† These authors contributed equally to the work.

‡joint senior authors

* Correspondence author: Tao Dong (email: tao.dong@imm.ox.ac.uk)

**Abstract**

Development of SARS-CoV-2 vaccines and therapeutics will depend on understanding viral immunity. We studied T-cell memory in 42 patients following recovery from COVID-19 (28 mild, 14 severe, 16 unexposed donors), using IFN-γ-based assays with peptides spanning SARS-CoV-2 except ORF1. The breadth and magnitude of T-cell responses were significantly higher in severe compared to mild cases. Total and spike-specific T-cell responses correlated with spike-specific antibody responses. We identified 41 peptides containing $CD4^+$ and/or $CD8^+$ epitopes, including six immunodominant regions. Six optimised CD8+ epitopes were defined, with peptide-MHC-pentamer-positive cells displaying central- and effector-memory phenotype. In mild cases, higher proportions of SARS-CoV-2-specific CD8+ T-cells were observed. The identification of T-cell responses associated with milder disease, will support an understanding of protective immunity, and highlights the potential of including non-spike proteins within future COVID-19 vaccine design.

## Introduction

COVID-19 is caused by the recently emerged Severe Acute Respiratory Syndrome coronavirus-2 (SARS-CoV-2). Whilst the majority of COVID-19 infections are relatively mild, with recovery typically within two to three weeks[1, 2], a significant number of patients develop severe illness, which is postulated to be related to both an overactive immune response and viral-induced pathology[3, 4]. The role of T-cell immune responses in disease pathogenesis and longer-term protective immunity is currently poorly defined, but essential to understand in order to inform therapeutic interventions and vaccine design.

Currently, there are many ongoing vaccine trials, but it is unknown whether they will provide long lasting protective immunity. Most vaccines are designed to induce antibodies to the SARS-CoV-2 spike protein, but it is not yet known if this will be sufficient to induce full protective immunity to SARS-CoV-2[5,6, 7,8]. Studying natural immunity to the virus, including the role of SARS-CoV-2-specific T-cells is critical to fill the current knowledge gaps for improved vaccine design.

For many primary virus infections, it typically takes 7-10 days to prime and expand adaptive T-cell immune responses in order to control the virus[9]. This coincides with the typical time it takes for COVID-19 patients to either recover or develop severe illness. There is an incubation time of 4-7 days before symptom onset, and a further 7-10 days before individuals progress to severe disease[10]. Such a pattern of progression raises the possibility that a poor T cell response contributes to SARS-CoV-2 viral persistence and COVID-19 mortality, whereas strong T cell responses are protective in the majority of individuals.

Evidence supporting a role for T cells in COVID-19 protection and pathogenesis is currently incomplete and sometimes conflicting[3,11,12,13,14]. To date there have been few studies analysing SARS-CoV-2-specific T-cell responses and their role in disease progression [15],

101 although virus specific T cells have been shown to be protective in human influenza
102 infection[16]. In a study of $CD4^+$ and $CD8^+$ T-cell responses to SARS-CoV-2 in non-
103 hospitalised convalescent subjects, Grifoni *et al* found that all recovered subjects
104 established $CD4^+$ responses and 70% established $CD8^+$ memory responses to SARS-CoV-
105 2[17]. SARS-CoV-2-specific $CD4^+$ T-cell responses were also frequently observed in
106 unexposed subjects in their study, suggesting the possibility of pre-existing cross-reactive
107 immune memory to seasonal coronaviruses. In Singapore, Le Bert *et al*[18] found long lasting
108 T cell immunity to the original SARS coronavirus nucleoprotein (NP) in those that were
109 infected in 2003. These T cells cross-reacted with SARS-CoV-2 NP, and T cells cross
110 reactive with NSP7 and NSP13 of other coronaviruses were also present in those
111 uninfected with either SARS coronaviruses[18].
112
113 In the present study, the overall and immunodominant SARS-CoV-2–specific memory T-cell
114 response in subjects who had recovered from COVID-19 were evaluated *ex vivo* using
115 peptides spanning the full proteome of the SARS-CoV-2, except for ORF-1. Epitopes were
116 identified using two-dimensional matrix peptide pools and $CD4^+$ and $CD8^+$ T cell responses
117 were distinguished. The epitope specificity and HLA restriction of the dominant $CD8^+$ T-cell
118 responses were defined in *ex vivo* assays and using *in vitro* cultured short-term T-cell lines.
119 The *ex vivo* functions of SARS-CoV-2-specific T-cells specific for dominant epitopes were
120 evaluated by their intracellular cytokine production profiles. Broad, and frequently strong,
121 SARS-CoV-2 specific $CD4^+$ and $CD8^+$ T-cell responses were seen in the majority of
122 convalescent patients, with significantly larger overall T-cell responses in those that had
123 severe compared to mild disease. However, there was a greater proportion of $CD8^+$ T-cell
124 compared to $CD4^+$ T cell responses in mild cases with higher frequencies of multi-cytokine
125 production by matrix (M) and nucleoprotein (NP)-specific $CD8^+$ T-cells.

**Results:**

**Study subjects**

42 individuals were recruited following recovery from COVID-19, including 28 mild cases and 14 severe cases. In addition, 16 control individuals sampled in 2017-2019, before COVID-19 appeared, were studied in parallel. Supplementary Fig. 1 shows the participant characteristics. No significant differences in gender or age were noted between mild and severe groups. The SaO2/FiO2 ratio in severe cases ranged from 4.3 (where 4.5 would be the estimate for an individual with mild disease breathing ambient air) to 1.6 with the patients with critical disease having an estimate of 0.8 (median in severe group 3.8).

***Ex vivo* assessment of memory T cell responses specific to SARS-CoV-2**

PBMCs were tested for responses to a panel of 423 overlapping peptides spanning the SARS-CoV-2 proteome except ORF1, using *ex vivo* IFN-γ ELISpot assays. All overlapping peptides were placed into two 2-dimensional peptide matrices: a total of 61 peptide pools were tested, with 29 peptides in the first-dimension pools, as described in Supplementary Table 1. The majority of the participants exhibited SARS-CoV-2 memory T cell responses to at least one of the peptides. The overall distribution, magnitude and breadth of the IFN-γ responses against all SARS-CoV-2 virus peptides are shown in Fig. 1. There was no correlation between the T cell responses and the time that had elapsed from symptom development (Supplementary Fig. 2). No *ex vivo* IFN-γ-producing SARS-CoV-2-specific T cell responses were observed in healthy volunteers, who were all sampled before any chance of exposure, but in those with appropriate HLA types, T cell responses were observed to influenza virus, EBV, CMV (FEC) using pools of known T cell epitopes as well as PHA as positive controls (Supplementary Fig. 3). The breadth and magnitude of the T cell responses varied considerably between individuals. T cell responses were detected against epitopes distributed across a wide variety of virus proteins. Significantly higher

magnitude (p=0.002) and broader (p=0.002) overall T cell responses were observed in severe cases in comparison with mild cases, in particular for responses to spike (magnitude/breadth, p=0.021/0.016), membrane (magnitude/breadth, p<p+0.0003/p=0.033),ORF3(magnitude/breadth, p<0.0001/0.001) and ORF8 (magnitude/breadth, p=0.011/0.014) proteins (Fig. 2). Overall, we found strong and broad T cell memory responses were induced after recovery from COVID-19, and the breadth and magnitude of T-cell responses were significantly higher in severe compared to mild cases.

**Correlation with spike specific antibody responses**

The relationship between spike-specific, and overall T cell responses in association with spike-specific, receptor binding domain (RBD) and NP-specific antibody endpoint titres (EPTs) was assessed (Fig. 3). There were significant correlations between (a) spike-specific antibody titers and both overall T cell responses (p=0.0004/R=0.5185) and spike-specific T cell responses (p=0.0006/R=0.505); (b) RBD-specific antibody titers and both overall T cell responses (p=0.0004/R=0.5198) and spike-specific T cell responses (p=0.0004/R=0.5189); and (c) NP-specific antibody titers and both overall T cell responses (p=0.0015/R=0.4738) and spike-specific T cell responses (p=0.007/R=0.412). However, there was no significant association between NP-specific antibody titers and NP-specific T cell responses (p=0.067/R= 0.286); (Fig. 3a-c; and Supplementary Fig. 4). Moreover, significantly higher level of spike, RBD and NP EPTs were observed in severe cases in comparison with mild cases (Fig. 3d). It was noted that some individuals had low RBD-specific antibodies (Fig. 3b), yet had detectable spike-specific antibodies (Fig. 3a), suggesting that antibodies were able to target non-RBD regions of spike – these are under further investigation. Thus total and spike-specific T-cell responses were found to be correlated with spike-specific antibody responses.

**Distribution of SARS-CoV-2–specific $CD4^+$ and $CD8^+$ memory T cell responses**

Having identified overall T cell responses to SARS-CoV-2 peptides, the responses detected against positive peptide pools were characterized by flow cytometry for peptide recognition by $CD4^+$ or $CD8^+$ T cell subsets and for intracellular production of IFN-γ, TNF- and IL-2 after stimulation (Fig. 4a-b and Supplementary Fig. 5). A greater proportion of the T cell responses to spike (p=0.0268) and M/NP (p=0.02) were contributed to by CD8+ T cells in those with mild disease compared to those with severe disease (Fig. 4c, Supplementary Fig. 6a). Differential subsets of SARS-CoV-2-specific T cells therefore associate with clinical outcome.

**Evaluation of the polyfunctionality of T cells responding to SARS-CoV-2 peptides**

Multi-cytokine analysis revealed patterns of IFN-γ, TNF and IL-2 production by $CD4^+$ and $CD8^+$ T cells in both mild and severe cases (Fig. 5a), For 22 individuals tested, both $CD4^+$ and $CD8^+$ antigen-specific-T cells produced least one of these three cytokines and others in combination. $CD8^+$ but not $CD4^+$ T cells targeting different virus proteins showed different cytokine profiles, with the M/NP-specific $CD8^+$ T cells showing wider functionality than T cells targeting spike protein (p=0.0231, Fig. 5b and Supplementary Fig. 6b). Furthermore, there were a greater proportion of multifunctional M/NP-specific $CD8^+$ T cells compared to spike-specific T cells in those that had mild disease (p=0.0037), but not in those that had severe disease (p=0.3823). In contrast to observations seen in influenza virus infection[19] , we did not observe significant differences in the cytotoxic potential (as indicated by expression of the degranulation marker CD107a) in patients with mild and severe disease (Fig. 5c); and we observed very few $CD107a^+$ $CD4^+$ T cells overall, suggesting cytotoxic $CD4^+$ T cells might not be a major contributor to virus clearance.

**Identification of SARS-CoV-2 specific T cell peptides containing epitopes**

IFN-γ ELISpot assays were performed with candidate peptides identified from the 2-dimensional matrix analysis in 34 subjects. A total of 41 peptides containing SARS-CoV-2 T

cell epitope regions were recognized by COVID-19 convalescent subjects, 18 from spike, 10 from NP, 6 from membrane and 7 from ORF proteins. Strikingly, 6 dominant 18mer peptides were recognised by 6 or more of 34 subjects tested (Table 1). NP-16 was recognised by 12/34 (35%) subjects tested and contained at least two epitopes which recognised by either CD4+ T cells or CD8+ T cells.

M-24 was recognised by 16/34 subjects (47%) tested and contained one or more $CD4^+$ T cell epitopes. Peptide M-20 was recognised by 11/34 subjects tested (32%) and contained one or more $CD4^+$ T cell epitopes. 3 dominant spike peptides were also identified, with S-34 recognised by 10/34 subjects (29%) containing both $CD4^+$ and $CD8^+$ T cell epitopes, and a further two spike peptides S-151 and S-174 were recognised by 8/34 and 6/34 subjects (24% and 18%), both containing $CD4^+$ T cell epitopes.

Those dominant responses were further confirmed by *ex-vivo* assays and by using cultured short-term T cell lines. Supplementary Fig. 7 illustrates examples of FACS plots from intracellular cytokine staining (ICS) when short-term T cell lines were stimulated with single peptides containing epitopes. $CD4^+$ T cells elicited strong responses against dominant spike peptides and M peptides, whereas cells targeting two NP dominant peptides were $CD8^+$ T cells. The optimal epitopes within the long peptides recognized by dominant CD8+ T cells and their HLA restriction, matched to the donor's HLA type, were predicted using the IEDB analysis resource (http://tools.iedb.org/mhci). The best predicted epitope sequences are shown in supplementary Table 2.

A set of previously defined SARS epitopes[20] with identical sequences to SARS-CoV-2 were also tested by ELISpot assay (Supplementary Table 3), Most of those peptides did not elicit any positive responses in 42 COVID-19 recovered subjects, apart from two NP epitope peptides (N-E-3 MEVTPSGTWL and N-E-11 LLNKHIDAYKTFPPTEPK) and one spike epitope peptide (S-E-19 QLIRAAEIRASANLAATK) . N-E-11, which is identical to peptide

NP-51, shares the sequence with two other known HLA-A*0201 restricted SARS epitopes (N-E-1 ILLNKHID and N-E-5 ILLNKHIDA). Interestingly, one of the responders to this peptide did not carry the HLA-A*0201 allele (Table 1), indicating this peptide may contain a different SARS-CoV-2 epitope presented by a different HLA molecule. Whereas these NP epitopes are targeted by $CD8^+$ T cells, we also detected a $CD4^+$ T cell response targeting SARS spike epitope S-E-19 which spans between the overlapping peptides of S-203 and S-204. This peptide is known to be presented by HLA-DRB1*0401 in SARS infection.

The optimal peptide sequences and their HLA restrictions were confirmed by generating short term T cell lines and clones, which were tested in ELIspot assays by co-culturing with peptide loaded HLA matched and unmatched immortalized B lymphoblastoid cell lines (BCLs) as previously described[21]. In total 6 CD8+ T cell epitopes restricted by HLA-A*0101, A*0301, A*1101, B*0702, B*4001 and B*2705 were confirmed (Table 2). HLA-peptide pentamers were synthesized comprising 5 peptides bound to the appropriate HLA class I molecules. T cell staining was verified by flowcytometry (Fig. 6) and their phenotypes were determined (Fig. 7). A pentameric HLA-A*0201 with the spike epitope reported by Shomuradova et al[22], was synthesised. Only one out of six HLA-A*0201-positive donors showed detectable staining, but at a very low frequency. The majority of pentamer stained SARS-Cov-2 specific $CD8^+$ T cells exhibited central memory (20.7%±8.4%) or effector memory phenotypes (50.3%±13.3%) (Fig. 7) and early (CD27+CD28+, 43.8%±20.9%) or intermediate (CD27+CD28-, 49.3%±21.0%) differentiation phenotypes. Overall, multiple peptides containing epitopes and immunodominant regions were defined from 42 subjects who had recovered from COVID-19. The regions were located in the majority of SARS-CoV-2 structural and non-structural proteins including spike, M, NP and ORF proteins, with CD8+ T cells exhibiting central memory and effector memory phenotype.

**Discussion**

This study demonstrates the presence of robust memory T cell responses specific for SARS-CoV-2 in the blood of donors who have recovered from Covid-19. The broader and stronger SARS-CoV-2 specific T cell responses in patients who had severe disease may be the result of higher viral loads and may reflect a poorly functioning early T cell response that failed to control the virus, in addition to other factors such as direct virus-induced pathology associated with larger viral inoculums or poorer innate immunity. Alternatively, it is possible that the T cell response was itself harmful and contributes to disease severity. Consistent with recent reports from Grifoni *et al* and *Sekine* et al [17, 23], a particularly high frequency of spike protein-specific $CD4^+$ T cell responses was observed in patients who had recovered from COVID-19. This is very similar to influenza virus infection, where viral surface hemagglutinin (HA) elicited mostly $CD4^+$ T cell responses, whereas the majority of $CD8^+$ T cell responses were specific to viral internal proteins [24]. Understanding the roles of different subsets of T cells in protection or pathogenesis is a crucial question for COVID-19. The timing and strength of the first T cell responses, could be critical in determining this balance at an early stage of the infection.

Among the 41 peptides containing T cell epitopes that were identified in this study, six immunodominant epitope groups (peptides) were frequently targeted by T cells in many donors, including three in spike (29%, 24%, 18%), two in membrane protein (32%, 47%) and one in nucleoprotein (35%). The immunodominant peptide regions identified here may include multiple epitopes restricted by different HLAs (both class I and II, such as S-34 and NP16) with immunodominance preferences imposed by the antigen processing pathways. Whether or not these dominant responses play a role in immune protection merits further investigation in larger prospective cohorts.

A higher proportion of CD8+ T cell responses was observed in mild disease, suggesting the potential protective role of CD8+ T cell responses in mild disease or pathogenic role of CD4+ T cell responses in severe disease which merits further investigation.

The majority of pentamer-binding $CD8^+$ T cells were effector memory and central memory with early and intermediate differentiation phenotypes, with functional potential on antigen re-exposure. Because the number of donors studied was limited and they would likely show diverse TCRs, peptide/MHC affinities and antigen sensitivities for the different epitopes, it was not possible to make a detailed analysis comparing mild and severe cases. However, the groundwork, including epitope identification, was laid for future studies that can address this important issue.

Multiple strong dominant T cell responses were seen in study subjects, specific for the M and NP proteins. Dominant epitope regions within NP (NP-16) were detected in 35% of study subjects and M (M-20 and M24) were detected in 32% and 47%. In addition, a higher proportion of multi-cytokine producing M/NP-specific compared to spike-specific $CD8^+$ T cells was observed in subjects who had recovered from mild disease. A similar trend was also observed in severe cases, although was not significant possibly due to fewer cases. These data strongly suggest NP and M have potential for inclusion within future vaccines so as to stimulate strong effector T cell responses. Furthermore, T cells responding to these antigens may be more cross-reactive [18].

IFN-□ producing SARS-CoV-2 specific T cell responses were not observed in 16 healthy unexposed volunteers differing from recently published reoorts by Grifoni *et al*[17] and Braun *et al*[25], both of which used peptide stimulated induction of activation markers (AIM) assays. On the other hand, in a recent immunogenicity study of a recombinant adenovirus type-5 (Ad5) vectored COVID-19 vaccine human phase I trial in 108 volunteers without pre-exposure to COVID-19), spike-specific T cell responses, measured IFN-□□ELISpot and intracellular cytokine stimulation (ICS) assays, were not found before vaccination[6]. These differences could result from differences in sensitivity of the detection methods, AIM versus.

IFN-□ production assays. IFN-□ -ELISpot and ICS are well-established methods for evaluating antigen specific T cells, used in different virus infections and vaccine studies, that have direct functional relevance [24, 26, 27, 28]. The AIM assay is more recently developed assay, capable of detecting early responding T cells, that is independent of cytokine production. Both methods are valid but differ in sensitivity and possible functional relevance. However, it is also possible that different circulating coronaviruses have been previously present in the different geographical populations studied, giving cross reactive responses in some regions but not others, as suggested by Le Bert et al[18] . These T-cell cross reacting viruses could include not only SARS-CoV-1 and human "common cold" coronaviruses, but also other unknown coronaviruses of animal origin. It is also known that very sensitive assays can detect not only pre-existing naïve antigen specific $CD4^+$ T cells but also memory $CD4^+$ T cells. The latter are potentially primed by other microbes that cross react with viruses as diverse as CMV, HIV-1 and Ebolavirus in most unexposed humans [29, 30]. Therefore, similar findings with SARS-CoV-2 peptides do not necessarily mean the T cells were primed by previous infecting coronaviruses. Indeed, the implications of pre-existing cross-reactivity to seasonal coronavirus and other viruses for COVID-19 immunity merits further detailed investigation as nicely highlighted by *Sette A and Crotty S*[31] .

This study focuses on T cell responses in PBMC. There remains a lack of understanding of memory T cells (Trm) at the site of infection, which is likely providing the most potent protection as observed in influenza virus infection[32]. It is possible that the hierarchy of immunodominant circulating blood memory T cell pools may not exactly reflect that of Trm in the lung[17, 33, 34]. Therefore, understanding the features of tissue resident memory T cells and their association with disease severity will be critical and also merits further investigation.

Taken together, this study has demonstrated strong and broad SARS-CoV-2-specific $CD4^+$ and $CD8^+$ T cell responses in the majority of humans who had recovered from COVID-19.

The immunodominant epitope regions and peptides containing T cell epitopes identified in this study will provide critical tools to study the contribution of SARS-CoV-19 specific T cells in protection and immune pathology. Identification of non-spike dominant $CD8^+$ T cell epitopes, suggests the potential importance of including of non-spike protein such as NP, M and ORFs into future vaccine designs.

**Acknowledgments**

We are grateful to all of the participants for donating their samples and data for these analyses, and the research teams involved in the consenting, recruitment and sampling of these participants.

This work is supported by UK Medical Research Council (T.D, G.O, Y.P, M.S, G.N, Y-LC); Chinese Academy of Medical Sciences (CAMS) Innovation Fund for Medical Sciences (CIFMS), China (grant number: 2018-I2M-2-002)(T.D, Y.P, X.Y, G.L, D.D, D.I.S, J.M, G.R.S); National Institutes of Health, National Key R&D Program of China (2020YFE0202400) (T.D, Y.Z, R.J); China Scholarship Councile (Z.Y, G.L, C.L); The National Institute for Health Research [award CO-CIN-01](M.G.S); the Medical Research Council [grant MC_PC_19059](M.G.S); Wellcome Trust and Department for International Development [215091/Z/18/Z](M.G.S); the Bill and Melinda Gates Foundation [OPP1209135](MGS). The study is also funded by the NIHR Oxford Biomedical Research Centre (L.P.H, G.O, P.K, E.B, G.R.S), Senior Investigator Award (G.O) and Clinical Research Network (G.O) and Schmidt Futures(G.R.S); Health Protection Research Unit in Respiratory Infections NIHR200927 /WHRG_P82523(P.O) ; NIHR Senior Investigator Award, NIHR201385 / WHRR P84026(P.O); Imperial College Biomedical Research Centre , IS-BRC-1215-20013(P.O); National Institute of Allergy and Infectious Disease (Consortium for HIV/AIDS Vaccine Development UM1 AI 144371 (P.B and A.M) and R01 AI 118549 (PB). L.T, P.K and P.S are supported by the National Institute for Health

Research Health Protection Research Unit (NIHR HPRU) in Emerging and Zoonotic Infections [NIHR200907] at University of Liverpool in partnership with Public Health England (PHE), in collaboration with Liverpool School of Tropical Medicine and the University of Oxford. L.T is based at the University of Liverpool. P.K and P.S are based at the University of Oxford. L.T , Td.S and A.A.A are supported by the Wellcome Trust [grant numbers 205228/Z/16/Z (L.T) , 110058/Z/15/Z (Td.S) and 206377 (A.A.A). G.R.S is supported as a Wellcome Trust Senior Investigator (grant 095541/A/11/Z). PB and A.M are Jenner Institute Investigators.

This work uses data provided by patients and collected by the NHS as part of their care and support #DataSavesLives.

The views expressed are those of the authors and not necessarily those of the Department of Health and Social Care, DID, NIHR, MRC, Wellcome Trust or PHE

**Author Contribution:** T.D and G.O conceptualized the project, T.D, Y.P designed and supervised T cell experiments, J.M and G.R.S designed antibody experiments; Y.P, G.L, X.Y, Z.Y,D.D performed all T cell experiments; W.D, J.M, P.S, C.L, C.L.C, J.S.C, Y.Z, D.I.S, G.P, J.G, A.A.A,O.B,D.H, B.W and D.S.K performed Spike, RBD and NP EPTs experiments; T.R performed HLA typing; J.K, A.M, T.L, R.L, P.K , L.T, T.D.S, M.G.S, C.P.C, S.C.M, J. K.B, P.O established clinical cohorts and collected clinical sample and data; K.S, P.T, P.Z, C.D, J.R, P.S, P.S, D.W, U.R, Y.L.C, W.P, P.B, J.F, M.A.A, S.D, M.S, E.B, G.K, P.G, Y.Z, R.J, L.P.H provided critical reagents and technical assistance; Y.P, G.L, X.Y, Z.Y,D.D, W.D, P.Z, J.M analysed data, T.D wrote the original draft. G.O, J.K, A.M, P.B, P.K, P.O, L.T., G.R.S, R.C, P.S, M.G.S, B.M.K,C.P.C reviewed and edited the manuscript and Figures.

**Oxford Immunology Network Covid-19 response: T cell Immunity Team – additional contributors**

Barbara Kronsteiner, Anthony Brown , Emily Adland , Patpong Rongkard , Anna Csala , Helen Brown , Nicola Robinson, Panagiota Zacharopoulou , Vinicius Adriano , Prabhjeet Phalora , Oliver Sampson , Carl-Philipp Hackstein , Nicholas Lim , Matt Edmans , Senthil Chinnakannan , Rachael Brown , Ali Amini , Mathew Jones , Mohammad Ali , Timothy Donnison , Matt Pace , Ane Ogbe , Donal Skelly , Elizabeth Stafford , Helen Fletcher , Lian Lee , Prathiba Kurupati , Rachel Etherington , Nicholas Provine, Hashem Koohy, Chloe Hyun-Jung Lee.

**ISARIC 4C Investigators**

Consortium Lead Investigator: J Kenneth Baillie, Chief Investigator Malcolm G Semple Co-Lead Investigator Peter JM Openshaw. ISARIC Clinical Coordinator Gail Carson. Co-Investigators: Beatrice Alex, Benjamin Bach, Wendy S Barclay, Debby Bogaert, Meera Chand, Graham S Cooke, Annemarie B Docherty, Jake Dunning, Ana da Silva Filipe, Tom Fletcher, Christopher A Green, Ewen M Harrison, Julian A Hiscox, Antonia Ying Wai Ho, Peter W Horby, Samreen Ijaz, Saye Khoo, Paul Klenerman, Andrew Law, Wei Shen Lim, Alexander, J Mentzer, Laura Merson, Alison M Meynert, Mahdad Noursadeghi, Shona C Moore, Massimo Palmarini, William A Paxton, Georgios Pollakis, Nicholas Price, Andrew Rambaut, David L Robertson, Clark D Russell, Vanessa Sancho-Shimizu, Janet T Scott, Louise Sigfrid, Tom Solomon, Shiranee Sriskandan, David Stuart, Charlotte Summers, Richard S Tedder, Emma C Thomson, Ryan S Thwaites, Lance CW Turtle, Maria Zambon. Project Managers Hayley Hardwick, Chloe Donohue, Jane Ewins, Wilna Oosthuyzen, Fiona Griffiths. Data Analysts: Lisa Norman, Riinu Pius, Tom M Drake, Cameron J Fairfield, Stephen Knight, Kenneth A Mclean, Derek Murphy, Catherine A Shaw. Data and Information System Manager: Jo Dalton, Michelle Girvan, Egle Saviciute, Stephanie Roberts Janet Harrison, Laura Marsh, Marie Connor. Data integration and presentation: Gary Leeming, Andrew Law, Ross Hendry. Material Management: William Greenhalf, Victoria Shaw, Sarah

McDonald. Outbreak Laboratory Volunteers: Katie A. Ahmed, Jane A Armstrong, Milton Ashworth, Innocent G Asiimwe, Siddharth Bakshi, Samantha L Barlow, Laura Booth, Benjamin Brennan, Katie Bullock, Benjamin WA Catterall, Jordan J Clark, Emily A Clarke, Sarah Cole, Louise Cooper, Helen Cox, Christopher Davis, Oslem Dincarslan, Chris Dunn, Philip Dyer, Angela Elliott, Anthony Evans, Lewis WS Fisher, Terry Foster, Isabel Garcia-Dorival, Willliam Greenhalf, Philip Gunning, Catherine Hartley, Antonia Ho, Rebecca L Jensen, Christopher B Jones, Trevor R Jones, Shadia Khandaker, Katharine King, Robyn T. Kiy, Chrysa Koukorava, Annette Lake, Suzannah Lant, Diane Latawiec, L Lavelle-Langham, Daniella Lefteri, Lauren Lett, Lucia A Livoti, Maria Mancini, Sarah McDonald, Laurence McEvoy, John McLauchlan, Soeren Metelmann, Nahida S Miah, Joanna Middleton, Joyce Mitchell, Shona C Moore, Ellen G Murphy, Rebekah Penrice-Randal, Jack Pilgrim, Tessa Prince, Will Reynolds, P. Matthew Ridley, Debby Sales, Victoria E Shaw, Rebecca K Shears, Benjamin Small, Krishanthi S Subramaniam, Agnieska Szemiel, Aislynn Taggart, Jolanta Tanianis, Jordan Thomas, Erwan Trochu, Libby van Tonder, Eve Wilcock, J. Eunice Zhang. Local Principal Investigators: Kayode Adeniji, Daniel Agranoff, Ken Agwuh, Dhiraj Ail, Ana Alegria, Brian Angus, Abdul Ashish, Dougal Atkinson, Shahedal Bari, Gavin Barlow, Stella Barnass, Nicholas Barrett, Christopher Bassford, David Baxter, Michael Beadsworth, Jolanta Bernatoniene, John Berridge , Nicola Best , Pieter Bothma, David Brealey, Robin Brittain-Long, Naomi Bulteel, Tom Burden , Andrew Burtenshaw, Vikki Caruth, David Chadwick, Duncan Chambler, Nigel Chee, Jenny Child, Srikanth Chukkambotla, Tom Clark, Paul Collini, Catherine Cosgrove, Jason Cupitt, Maria-Teresa Cutino-Moguel, Paul Dark, Chris Dawson, Samir Dervisevic, Phil Donnison, Sam Douthwaite, Ingrid DuRand, Ahilanadan Dushianthan, Tristan Dyer, Cariad Evans , Chi Eziefula, Chrisopher Fegan, Adam Finn, Duncan Fullerton, Sanjeev Garg, Sanjeev Garg, Atul Garg, Jo Godden, Arthur Goldsmith, Clive Graham, Elaine Hardy, Stuart Hartshorn, Daniel Harvey, Peter Havalda, Daniel B Hawcutt, Maria Hobrok, Luke Hodgson, Anita Holme, Anil Hormis, Michael Jacobs, Susan Jain, Paul Jennings, Agilan Kaliappan, Vidya Kasipandian, Stephen Kegg, Michael Kelsey, Jason Kendall, Caroline Kerrison, Ian Kerslake, Oliver Koch, Gouri Koduri, George Koshy ,

Shondipon Laha, Susan Larkin, Tamas Leiner, Patrick Lillie, James Limb, Vanessa Linnett, Jeff Little, Michael MacMahon, Emily MacNaughton, Ravish Mankregod, Huw Masson , Elijah Matovu, Katherine McCullough, Ruth McEwen , Manjula Meda, Gary Mills , Jane Minton, Mariyam Mirfenderesky, Kavya Mohandas, Quen Mok, James Moon, Elinoor Moore, Patrick Morgan, Craig Morris, Katherine Mortimore, Samuel Moses, Mbiye Mpenge, Rohinton Mulla, Michael Murphy, Megan Nagel, Thapas Nagarajan, Mark Nelson, Igor Otahal, Mark Pais, Selva Panchatsharam, Hassan Paraiso, Brij Patel, Justin Pepperell, Mark Peters, Mandeep Phull , Stefania Pintus, Jagtur Singh Pooni, Frank Post, David Price, Rachel Prout, Nikolas Rae, Henrik Reschreiter, Tim Reynolds, Neil Richardson, Mark Roberts, Devender Roberts, Alistair Rose, Guy Rousseau, Brendan Ryan, Taranprit Saluja, Aarti Shah, Prad Shanmuga, Anil Sharma, Anna Shawcross, Jeremy Sizer, Richard Smith, Catherine Snelson, Nick Spittle, Nikki Staines , Tom Stambach, Richard Stewart, Pradeep Subudhi, Tamas Szakmany, Kate Tatham, Jo Thomas, Chris Thompson, Robert Thompson, Ascanio Tridente, Darell Tupper - Carey, Mary Twagira, Andrew Ustianowski, Nick Vallotton, Lisa Vincent-Smith, Shico Visuvanathan , Alan Vuylsteke, Sam Waddy, Rachel Wake, Andrew Walden, Ingeborg Welters, Tony Whitehouse, Paul Whittaker, Ashley Whittington, Meme Wijesinghe, Martin Williams, Lawrence Wilson, Sarah Wilson, Stephen Winchester, Martin Wiselka, Adam Wolverson, Daniel G Wooton, Andrew Workman, Bryan Yates, Peter Young.

All authors declare no competing interest

## References


1. Fehr A.R., P.S. Coronaviruses: An Overview of Their Replication and Pathogenesis. *In: Maier H., Bickerton E., Britton P. (eds) Coronaviruses. Methods in Molecular Biology* **vol 1282**.

2. Perlman, S. & Netland, J. Coronaviruses post-SARS: update on replication and pathogenesis. *Nat Rev Microbiol* **7**, 439-450 (2009).

3. Xu, Z. *et al.* Pathological findings of COVID-19 associated with acute respiratory distress syndrome. *Lancet Respir Med* **8**, 420-422 (2020).

4. Guan, W.J. *et al.* Clinical Characteristics of Coronavirus Disease 2019 in China. *N Engl J Med* (2020).

5. Yu, J. *et al.* DNA vaccine protection against SARS-CoV-2 in rhesus macaques. *Science* (2020).

6. Zhu, F.C. *et al.* Safety, tolerability, and immunogenicity of a recombinant adenovirus type-5 vectored COVID-19 vaccine: a dose-escalation, open-label, non-randomised, first-in-human trial. *Lancet* **395**, 1845-1854 (2020).

7. van Doremalen, N. *et al.* ChAdOx1 nCoV-19 vaccination prevents SARS-CoV-2 pneumonia in rhesus macaques. *bioRxiv*, 2020.2005.2013.093195 (2020).

8. Folegatti, P.M. *et al.* Safety and immunogenicity of the ChAdOx1 nCoV-19 vaccine against SARS-CoV-2: a preliminary report of a phase 1/2, single-blind, randomised controlled trial. *Lancet* (2020).

9. St John, A.L. & Rathore, A.P.S. Adaptive immune responses to primary and secondary dengue virus infections. *Nat Rev Immunol* **19**, 218-230 (2019).

10. Huang, C. *et al.* Clinical features of patients infected with 2019 novel coronavirus in Wuhan, China. *Lancet* **395**, 497-506 (2020).

11. Liao, M. *et al.* Single-cell landscape of bronchoalveolar immune cells in patients with COVID-19. *Nat Med* (2020).

12. chen, y. *et al.* The Novel Severe Acute Respiratory Syndrome Coronavirus 2 (SARS-CoV-2) Directly Decimates Human Spleens and Lymph Nodes. *medRxiv*, 2020.2003.2027.20045427 (2020).

13. Diao, B. *et al.* Reduction and Functional Exhaustion of T Cells in Patients With Coronavirus Disease 2019 (COVID-19). *Front Immunol* **11**, 827 (2020).

14. Pereira, B.I. *et al.* Sestrins induce natural killer function in senescent-like CD8(+) T cells. *Nat Immunol* **21**, 684-694 (2020).

15. Ni, L. *et al.* Detection of SARS-CoV-2-Specific Humoral and Cellular Immunity in COVID-19 Convalescent Individuals. *Immunity* (2020).

16. Hayward, A.C. *et al.* Natural T Cell-mediated Protection against Seasonal and Pandemic Influenza. Results of the Flu Watch Cohort Study. *Am J Respir Crit Care Med* **191**, 1422-1431 (2015).

17. Grifoni, A. *et al.* Targets of T Cell Responses to SARS-CoV-2 Coronavirus in Humans with COVID-19 Disease and Unexposed Individuals. *Cell* **181**, 1489-1501 e1415 (2020).

18. Le Bert, N. *et al.* SARS-CoV-2-specific T cell immunity in cases of COVID-19 and SARS, and uninfected controls. *Nature* (2020).

19. Wilkinson, T.M. *et al.* Preexisting influenza-specific CD4+ T cells correlate with disease protection against influenza challenge in humans. *Nat Med* **18**, 274-280 (2012).

20. Ahmed, S.F., Quadeer, A.A. & McKay, M.R. Preliminary Identification of Potential Vaccine Targets for the COVID-19 Coronavirus (SARS-CoV-2) Based on SARS-CoV Immunological Studies. *Viruses* **12** (2020).

21. Ogg, G.S. *et al.* Four novel cytotoxic T-lymphocyte epitopes in the highly conserved major homology region of HIV-1 Gag, restricted through B*4402, B*1801, A*2601, B*70 (B*1509). *AIDS* **12**, 1561-1563 (1998).

22. Shomuradova, A.S. *et al.* SARS-CoV-2 epitopes are recognized by a public and diverse repertoire of human T-cell receptors. *medRxiv*, 2020.2005.2020.20107813 (2020).

23. Sekine, T. *et al.* Robust T cell immunity in convalescent individuals with asymptomatic or mild COVID-19. *bioRxiv*, 2020.2006.2029.174888 (2020).

24. Lee, L.Y. *et al.* Memory T cells established by seasonal human influenza A infection cross-react with avian influenza A (H5N1) in healthy individuals. *J Clin Invest* **118**, 3478-3490 (2008).

25. Braun, J. *et al.* Presence of SARS-CoV-2 reactive T cells in COVID-19 patients and healthy donors. *medRxiv*, 2020.2004.2017.20061440 (2020).

26. Li, C.K. *et al.* T cell responses to whole SARS coronavirus in humans. *J Immunol* **181**, 5490-5500 (2008).

27. Powell, T.J. *et al.* Identification of H5N1-specific T-cell responses in a high-risk cohort in vietnam indicates the existence of potential asymptomatic infections. *J Infect Dis* **205**, 20-27 (2012).

28. Dong, T. *et al.* Extensive HLA-driven viral diversity following a narrow-source HIV-1 outbreak in rural China. *Blood* **118**, 98-106 (2011).

29. Su, L.F. & Davis, M.M. Antiviral memory phenotype T cells in unexposed adults. *Immunol Rev* **255**, 95-109 (2013).

30. Campion, S.L. *et al.* Proteome-wide analysis of HIV-specific naive and memory CD4(+) T cells in unexposed blood donors. *J Exp Med* **211**, 1273-1280 (2014).

31. Sette, A. & Crotty, S. Pre-existing immunity to SARS-CoV-2: the knowns and unknowns. *Nat Rev Immunol* (2020).

32. Pizzolla, A. *et al.* Resident memory CD8(+) T cells in the upper respiratory tract prevent pulmonary influenza virus infection. *Sci Immunol* **2** (2017).

33. Turner, D.L. *et al.* Lung niches for the generation and maintenance of tissue-resident memory T cells. *Mucosal Immunol* **7**, 501-510 (2014).

34. Yoshizawa, A. *et al.* TCR-pMHC encounter differentially regulates transcriptomes of tissue-resident CD8 T cells. *Eur J Immunol* **48**, 128-150 (2018).

606 **Table 1 Peptides containing T cell epitopes**

| | Peptide | Position | Amino Acid Sequence | CD4/CD8 Response | No of subjects responded |
|---|---|---|---|---|---|
| Spike | **S-34** | 166-180 | **CTFEYVSQPFLMDLE** | 4/8 | 10 |
| (n=18) | S-39 | 191-205 | EFVFKNIDGYFKIYS | na | 1 |
| | S-42 | 206-230 | KHTPINLVRDLPQGF | na | 1 |
| | S-43 | 211-225 | NLVRDLPQGFSALEP | na | 1 |
| | S-71 | 351-365 | YAWNRKRISNCVADY | 4 | 1 |
| | S-77 | 381-395 | GVSPTKLNDLCFTNV | 4 | 1 |
| | S-90 | 446-460 | GGNYNYLYRLFRKSN | na | 1 |
| | S-91 | 451-465 | YLYRLFRKSNLKPFE | na | 1 |
| | S-103 | 506-520 | VVLSFELLHAPATVC | 4 | 1 |
| | S-106 | 526-540 | GPKKSTNLVKNKCVN | 8 | 1 |
| | S-145 | 721-735 | SVTTEILPVSMTKTS | na | 1 |
| | S-150 | 746-760 | STECSNLLLQYGSFC | na | 1 |
| | **S-151** | 751-765 | **NLLLQYGSFCTQLNR** | 4 | 8 |
| | **S-161** | 801-815 | **NFSQILPDPSKPSKR** | 4 | 2 |
| | **S-174** | 866-880 | **TDEMIAQYTSALLAG** | 4 | 6 |
| | S-235 | 1171-1185 | GINASVVNIQKEIDR | na | 1 |
| | S-240 | 1196-1210 | LIDLQELGKYEQYI | na | 1 |
| | S-242 | 1206-1220 | YEQYIKWPWYIWLGF | na | 1 |
| | **NP-1** | 1-17 | **MSDNGPQNQRNAPRITF** | 8 | 3 |
| | **NP-2** | 8-25 | **NQRNAPRITFGGPSDSTG** | 8 | 3 |
| NP | NP-12 | 82-95 | DQIGYYRRATRRIR | na | 1 |
| (n=10) | NP-15 | 101-113 | MKDLSPRWYFYYL | na | 1 |
| | **NP-16** | 104-121 | **LSPRWYFYYLGTGPEAGL** | 4/8 | 12 |
| | NP-46 | 313-330 | AFFGMSRIGMEVTPSGTW | na | 1 |
| | NP-47 | 321-338 | GMEVTPSGTWLTYTGAIK | na | 1 |
| | **NP-48** | 329-346 | **TWLTYTGAIKLDDKDPNF** | 4 | 2 |
| | NP-50 | 344-361 | PNFKDQVILLNKHIDAYK | 4 | 1 |
| | **NP-51** | 352-369 | **LLNKHIDAYKTFPPTEPK** | 8 | 3 |
| | **M19** | 133-150 | **LLESELVIGAVILRGHLR** | na | 3 |
| M | **M-20** | 141-158 | **GAVILRGHLRIAGHHLGR** | 4 | 11 |
| (n=6) | **M-21** | 149-166 | **LRIAGHHLGRCDIKDLPK** | na | 3 |
| | **M-23** | 165-181 | **PKEITVATSRTLSYYKL** | na | 3 |
| | **M-24** | 172-188 | **TSRTLSYYKLGASQRVA** | 4 | 16 |
| | M-28 | 201-218 | IGNYKLNTDHSSSSDNIA | na | 1 |
| ORFs | ORF-3a-20 | 145-160 | YFLCWHTNCYDYCIPY | na | 1 |
| (n=7) | **ORF-3a-27** | 198-215 | **KDCVVLHSYFTSDYYQLY** | na | 3 |
| | **ORF-3a-28** | 206-225 | **YFTSDYYQLYSTQLSTDTGV** | 8 | 4 |
| | ORF-3a-30 | 224-243 | GVEHVTFFIYNKIVDEPEEH | na | 1 |
| | **ORF-7a-2** | 9-25 | **LITLATCELYHYQECVR** | na | 3 |
| | ORF-7a-7 | 46-63 | FHPLADNKFALTCFSTQF | na | 1 |
| | ORF-7a-10 | 69-86 | DGVKHVYQLRARSVSPKL | 4 | 1 |

607

608 Red highlights the overlaps of two adjacent peptides recognised by same subjects; Bold
609 indicates multiple donor responders; Peptides with underline are the 6 immunodominant
610 peptides. na: not available

**Table 2: List of identified optimal CD8 epitopes**

| Protein | Position | Epitope sequence | HLA Restriction |
|---|---|---|---|
| NP | 9-17 | QRNAPRITF | B*2705 |
| | 105-113 | SPRWYFYYL | B*0702 |
| | 322-331 | MEVTPSGTWL | B*4001 |
| | 362-370 | KTFPPTEPK | A*0301 |
| | 362-370 | KTFPPTEPK | A*1101 |
| ORF3a | 207-215 | FTSDYYQLY | A*0101 |

Location , sequence and HLA restriction of six identified SARS-CoV2 CD8 optimal epitopes.

## Figure Legends

**Fig. 1: Memory T cell responses specific to SARS-CoV-2 virus proteins in 42 convalescent SARS-CoV-2-infected patients.** 28 individuals had mild symptoms while 14 showed severe symptoms. PBMC were isolated and IFN-□ production was detected by ELISpot after incubation with SARS-CoV-2 peptides. a) Magnitude of IFN-□ T cell responses from each individual. Each bar shows the total T cell responses of each individual specific to all the SARS-CoV-2 protein peptides tested. Each colored segment represents the source protein corresponding to peptide pools eliciting IFN-γ T cell responses. b) Breadth of T cell responses from each individual. The breadth of T cell responses was calculated by the number of peptide pools in the first-dimension (total 29) cells responded to SFU spot forming units. Experiments were repeated in 35 subjects where sample availability permitted.

**Fig. 2: Comparison of magnitude and breadth of T cell response specific to each viral protein between convalescent patients with mild symptoms and severe symptoms.** PBMCs were isolated and IFN-□ production was detected by ELISpot after incubation with SARS-CoV-2 peptides. a) and b) illustrate the magnitude and the breadth of T cell response against each viral protein between the groups with mild symptoms (n=28) and with severe symptoms (n=14), respectively. Overall, magnitude/breadth: p=0.002/p=0.002; Spike, magnitude/breadth: p=0.021/0p=0.016; M, magnitude/breadth: p=0.0003/p=0.033; ORF3a, magnitude/breadth: p<0.0001/p=0.001); ORF8, magnitude/breadth: p=0.011/p=0.014). Data are presented as median with interquartile range. Mann-Whitney test was used for the analysis and two-tailed p value was calculated. *P<0.05, **P<0.01, ***P<0.001, ****P<0.001. SFU spot forming units;

**Fig. 3: Correlation of T cell responses against SARS-CoV-2 with Spike, RBD and NP-specific antibody responses.** a) EPTs-spike b) EPTs-RBD and c) EPTs-NP in association with overall T cell responses. Red dots represent the patients with severe symptoms

whereas the mild cases are shown as black dots. n=42. Spearman's rank correlation coefficient was used for the correlation analysis. d) Comparison of EPT-spike ($p<0.0001$), EPT-RBD ($p<0.0001$) and EPT-NP ($p=0.0004$) with mild symptoms (n=28) and severe symptoms (n=14). Data are presented as median with interquartile range and Mann-Whitney test was used for comparison. Two-tailed p value was calculated. *** $P<0.001$; **** $P<0.0001$
EPT: Endpoint titer

**Fig. 4: Distribution of SARS-CoV-2–specific $CD4^+$ and $CD8^+$ memory T cell responses**
Cytokine producing T cells were detected by ICS after incubation with SARS-CoV-2 peptides. a) and b) Flow cytometric plots represent $CD4^+$T cell and $CD8^+$ T cells expressing IFN-□ (x-axis),TNF (y-axis) and/or IL-2 (y-axis) upon stimulation with respective SARS-CoV-2 peptide pools in examples of mild and severe cases. c) Comparison of relative proportion of SARS-CoV-2 peptide pool-reactive $CD8^+$ T cells between mild (Spike, n=11; M/NP, n=14; ORF/Env, n=5; Overall: n=14) and severe cases (Spike, n=7; M/NP, n=7; ORF/Env, n=4; Overall, n=8). Spike, p=0.0268; M/NP, p=0.02; Overall, p=0.0159. The SARS-CoV-2 peptide pool-reactive $CD4^+$ or $CD8^+$ T cells were identified with at least one of the three cytokines detected: IFN-□, TNF and IL-2. Data shown are as median with interquartile range. Mann-Whitney test was used for the analysis. Two-tailed p value was calculated. * $P<0.05$

**Fig. 5: Cytokine profile of SARS-Cov-2-specific T cells.** Cytokine production of SARS-Cov-2-specific T cells was assessed by intracellular cytokine staining after incubation with SARS-CoV-2 peptides. a) Pie charts represent the relative proportions of $CD4^+$ or $CD8^+$ T cells producing, and the relative proportion of T cells producing one, two and three cytokines IFN-□, TNF and IL-2. Different colored segments represented different pattern of cytokine production. b) Comparison of the frequency of multifunctional $CD8^+$ T cells targeting Spike and M/NP. The open circles and squares represent T cell responses in mild cases and severe cases, respectively. Mild, p=0.0037; Severe, p=0.3823; Overall, p=0.0231. c) The relative frequencies of $CD4^+$ and $CD8^+$ T cells expressing CD107a after antigen-stimulation.

689 Data shown are from 14 subjects with mild symptoms and 8 with severe symptoms. Mann-
690 Whitney test was used for the analysis. Two-tailed p value was calculated. * P<0.05,
691 **P<0.01
692
693 **Fig. 6: Defined SARS-CoV-2-specific CD8 epitopes.** Examples of peptide-MHC Class I
694 pentamers staining ex-vivo with PBMCs (HLA-B0702, B4001, A1101, A0101 and A0201) or
695 with cultured cell lines (A0301), 11 donors were tested with positive Pentamer staining.
696
697 **Fig. 7: Memory phenotype and differentiation status of SARS-CoV-2-specific CD8+ T**
698 **cells.** PBMC were isolated and stained with peptide-MHC class I Pentameric complexes and
699 markers of T cell memory and differentiation. a) Representative FACS plots of gating for
700 different cell subsets b) and c) Expression of memory markers (CCR7 and CD45RA) and
701 differentiation markers (CD27 and CD28) on $CD8^+$ Pentamer+ T cells, respectively. n=7
702 donors. Data are presented as mean ± SEM.
703

## Materials and methods

### Ethical Statement

Patients were recruited from the John Radcliffe Hospital in Oxford, UK, between March and May 2020 by identification of patients hospitalised during the SARS-COV-2 pandemic and recruited into the Sepsis Immunomics and ISARIC WHO Clinical Characterisation Protocol UK (IRAS 260007 and IRAS126600). Patients were sampled at least 28 days from the start of their symptoms. Unexposed healthy adult donor samples were used from unrelated studies undertaken between 2017-early 2019. Written informed consent was obtained from all patients. Ethical approval was given by the South Central - Oxford C Research Ethics Committee in England (Ref 13/SC/0149), the Scotland A Research Ethics Committee (Ref 20/SS/0028), and the WHO Ethics Review Committee (RPC571 and RPC572, 25 April 2013).

### Clinical definitions

All patients were confirmed to have a test positive for SARS-CoV-2 using reverse transcriptase polymerase chain reaction (RT-PCR) from an upper respiratory tract (nose/throat) swab tested in accredited laboratories. The degree of severity was identified as mild, severe or critical infection according to recommendations from the World Health Organisation. Patients were classified as ‘mild’ if they did not require oxygen (that is, their oxygen saturations were greater than 93% on ambient air) or if their symptoms were managed at home. A large proportion of our mild cases were admitted to hospital for public health reasons during the early phase of the pandemic even though they had no medical reason to be admitted to hospital. Severe infection was defined as COVID-19 confirmed patients with one of the following conditions: respiratory distress with RR>30/min; blood oxygen saturation<93%; arterial oxygen partial pressure (PaO2) / fraction of inspired O2 (FiO2) <300mmHg; and critical infection was defined as respiratory failure requiring mechanical ventilation or shock; or other organ failures requiring admission

to ICU. Since the Severe classification could potentially include individuals spanning a wide spectrum of disease severity ranging from patients receiving oxygen through a nasal cannula through to non-invasive ventilation we also calculated the SaO2/FiO2 ratio at the height of patient illness as a quantitative marker of lung damage. This was calculated by dividing the oxygen saturation (as determined using a bedside pulse oximeter) by the fraction of inspired oxygen (21% for ambient air, 24% for nasal cannulae, 28% for simple face masks and 28, 35, 40 or 60% for Venturi face masks or precise measurements for non-invasive or invasive ventilation settings). Patients not requiring oxygen with oxygen saturations (if measured) greater than 93% on ambient air, or managed at home were classified as mild disease. Viral swab Ct values were not available for all patients. In addition, we have standardised all of our analyses to the days since symptom onset.

**Synthetic peptides**

A total of 423 15- to 18-mer peptides overlapping by 10 amino acid residues and spanning the full proteome of the SARS-CoV-2 except ORF-1 (Supplementary Table 1) were designed using software PeptGen (http://www.hiv.lanl.gov/content/sequence/PEPTGEN/peptgen.html) and synthesized (purity >75%; Proimmune).

27 previously defined SARS epitopes[20] were also synthesised (Supplementory Table 2).Pools of Cytomegalovirus (CMV),Epstein-Barr cirus (EBV) and influenza virus specific epitope peptides and The human immunodeficiency viruses (HIV) gag were also used as positive and negative controls.

**2-dimensional peptide matrix system**

The overlapping peptides spanning the SARS-CoV-2 were assigned into a 2-dimensional matrix system in which each peptide was represented in 2 different peptide pools. Each peptide pool contains no more than 16 individual peptides. The first dimension of the peptide matrix system was designed so that peptides from different source proteins were separated into different pools. (Supplemental Table 1).

760

761 ***Ex vivo* ELISpot assay**

762 IFN-γ ELISpot assays were performed using either freshly isolated or cryopreserved PBMCs
763 as described previously. No significant difference was observed between responses
764 generated by fresh or cryopreserved PBMCs as described previously[24, 35].

765

766 Overlapping peptides were pooled and then added to 200,000 PBMCs per test at the final
767 concentration of 2µg/mL for 16–18 h, the positive responses were confirmed by repeat
768 ELISPOT assays. To quantify antigen-specific responses, mean spots of the control wells
769 were subtracted from the positive wells, and the results expressed as spot forming units
770 (SFU)/$10^6$ PBMCs. Responses were considered positive if results were at least three times
771 the mean of the negative control wells and >25SFU/$10^6$PBMCs. If negative control wells
772 had >30SFU/$10^6$ PBMCs or positive control wells (PHA stimulation) were negative, the
773 results were excluded from further analysis.

774

775 **Determination of plasma binding to trimeric spike, RBD and NP by ELISA**

776 MAXISORP immunoplates (442404; NUNC) were coated with 0.125µg of StrepMAB-Classic
777 (2-1507-001;iba) , blocked with 2% skimmed milk in PBS for one hour and then incubated
778 with 50µL of 5µg/mL soluble trimeric Spike 2µg/mL or 2% skim milk in PBS. After one hour,
779 50 µL of serial two-fold dilutions of plasma, from 1:50 to 1:51200 in PBS containing 2%
780 skimmed milk were added followed by ALP-conjugated anti-human IgG (A9544; Sigma) at
781 1:10,000 dilution. The reaction was developed by the addition of PNPP substrate and
782 stopped with NaOH. The absorbance was measured at 405nm. Endpoint titers (EPTs) were
783 defined as reciprocal plasma dilutions that corresponded to two times the average OD
784 values obtained with mock. To determine EPTs to RBD and NP, immunoplates were coated
785 with 0.125ug of Tetra-His antibody (34670; QIAGEN) followed by 2µg/mL and 5µg/mL of
786 soluble RBD and NP, respectively.

**Intracellular cytokine staining (ICS)**

Intracellular cytokine staining was performed as described previously[36, 37] . Briefly, overnight rested PBMCs were stimulated with pooled or individual peptides at a final concentration of 10µg/mL for 1 h in the presence of 2µg/mL monoclonal antibodies CD28 and CD49d, and then for an additional 5h with GolgiPlug, GolgiStop and surface stained with PE-anti-CD107a. Dead cells were labelled using LIVE/DEAD™ Fixable Aqua dye from Invitrogen; surface markers including BUV395-anti-CD3, BUV737-anti-CD4, PerCP-Cy5.5-anti-CD8, BV510-anti-CD14 (Biolegend), BV510-anti-CD16 (Biolegend) and BV510-anti-CD19 (Biolegend) were stained. Cells were then washed, fixed with Cytofix/Cytoperm™ and stained with PE-Cy7-anti-IFNγ, APC-anti-TNFα (eBioscience), BV421-anti-IL-2 (Biolegend). Negative controls without peptide-stimulation were run for each sample. All reagents were from BD Bioscience unless otherwise stated. All samples were acquired on BD LSR Fortessa (BD Biosciences) flow cytometer and analyzed using FlowJo™ v.10 software (FlowJo LLC). Peptide pool-reactive $CD4^+$ or $CD8^+$ T cells with frequency lower than 0.05% of $CD4^+$ or $CD8^+$ T cells respectively were excluded for analysis. Cytokine responses were background subtracted individually prior to further analysis. To determine the frequency of different response patterns based on all possible combinations, Boolean gates were created using IFN-γ, TNF-α and IL-2. Cytokine responses were background subtracted individually prior to further analysis.

**Pentamer phenotyping**

Cryopreserved PBMCs were thawed as described above. A total of $1 \times 10^6$ live PBMCs were labeled with peptide-MHC class I Pentamer-PE (Proimmune, UK) and incubated for 15 min at 37°C. Dead cells were first labelled with LIVE/DEAD™ Fixable Aqua dye (Invitrogen) and then with surface markers CD3-BUV395, CD8-PerCP.Cy5.5, CD14-BV510 (Biolegend UK), CD16-BV510 (Biolegend UK), CD19-BV510 (Biolegend UK), CD28-BV711, CD27-APC-R700, CD45RA-APC-H7 and CCR7-PE-Dazzel 594 (Biolegend UK). All reagents were from

BD Bioscience unless otherwise stated. All samples were acquired on BD LSR Fortessa (BD Biosciences) flow cytometer and analyzed using FlowJo™ v.10 software (FlowJo LLC).

**Generating short-term T cell lines**

Short-term SARS-CoV-2-specific T cell lines were established as previously described [35]. Briefly, 3 × $10^6$ to 5 × $10^6$ PBMCs were pulsed as a pellet for 1 h at 37°C with 10 µM of peptides containing T cell epitope regions and cultured in R10 at 2 × $10^6$ cells per well in a 24-well Costar plate. IL-2 was added to a final concentration of 100U/mL on day 3 and cultured for further 10 -14 days.

**Statistical analysis**

Statistical analysis was performed with IBM SPSS Statistics 25 and Fig.s were made with GraphPad Prism 8. Chi-square tests were used to compare ratio difference between two groups. After testing for normality using Kolmogorov-Smirnov test, Independent-samples *t* test or Mann-Whitney U test was employed to compare variables between two groups. Correlations were performed via Spearman's rank correlation coefficient. Statistical significance was set at *P<0.05, **P<0.01, ***P<0.001 and ****P<0.0001. All the tests were 2-tailed.

**Life Sciences Reporting Summary**

Further information on research design is available in the Nature Research Reporting Summary linked to this article.

**Data availability**

Source data are provided with this paper. The corresponding author can be contacted for further information.

**Method-Only References:**

35. Peng, Y. *et al.* Boosted Influenza-Specific T Cell Responses after H5N1 Pandemic Live Attenuated Influenza Virus Vaccination. *Front Immunol* **6**, 287 (2015).

36. Lillie, P.J. *et al.* Preliminary assessment of the efficacy of a T-cell-based influenza vaccine, MVA-NP+M1, in humans. *Clin Infect Dis* **55**, 19-25 (2012).

37. de Silva, T.I. *et al.* Correlates of T-cell-mediated viral control and phenotype of CD8(+) T cells in HIV-2, a naturally contained human retroviral infection. *Blood* **121**, 4330-4339 (2013).

Figure 1

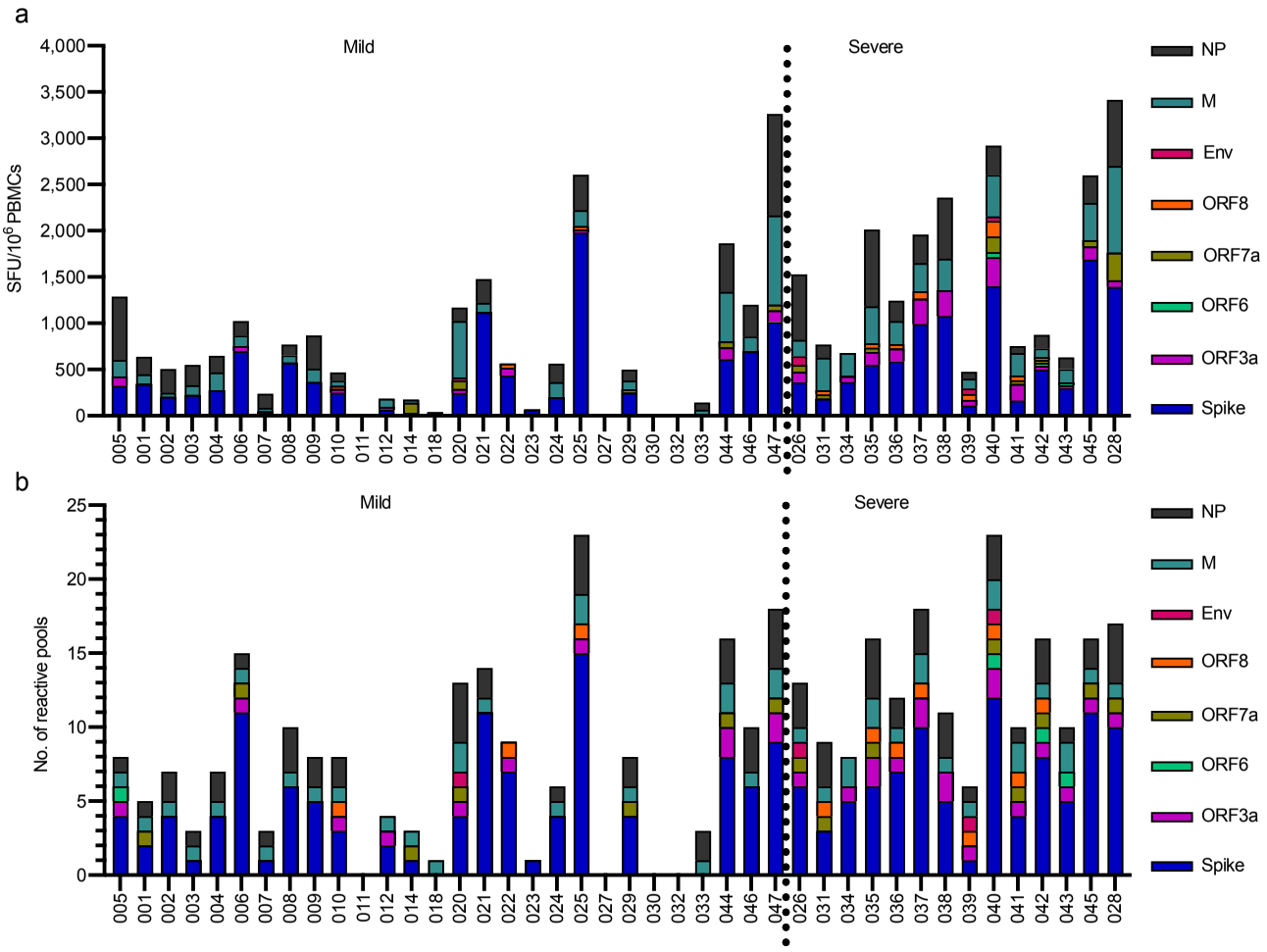
a
Mild
Severe
SFU/10^6 PBMCs
4,000
3,500
3,000
2,500
2,000
1,500
1,000
500
0
005 001 002 003 004 006 007 008 009 010 011 012 014 018 020 021 022 023 024 025 027 029 030 032 033 044 046 047 026 031 034 035 036 037 038 039 040 041 042 043 045 028
NP
M
Env
ORF8
ORF7a
ORF6
ORF3a
Spike
b
Mild
Severe
No. of reactive pools
25
20
15
10
5
0
005 001 002 003 004 006 007 008 009 010 011 012 014 018 020 021 022 023 024 025 027 029 030 032 033 044 046 047 026 031 034 035 036 037 038 039 040 041 042 043 045 028
NP
M
Env
ORF8
ORF7a
ORF6
ORF3a
Spike

Figure 2

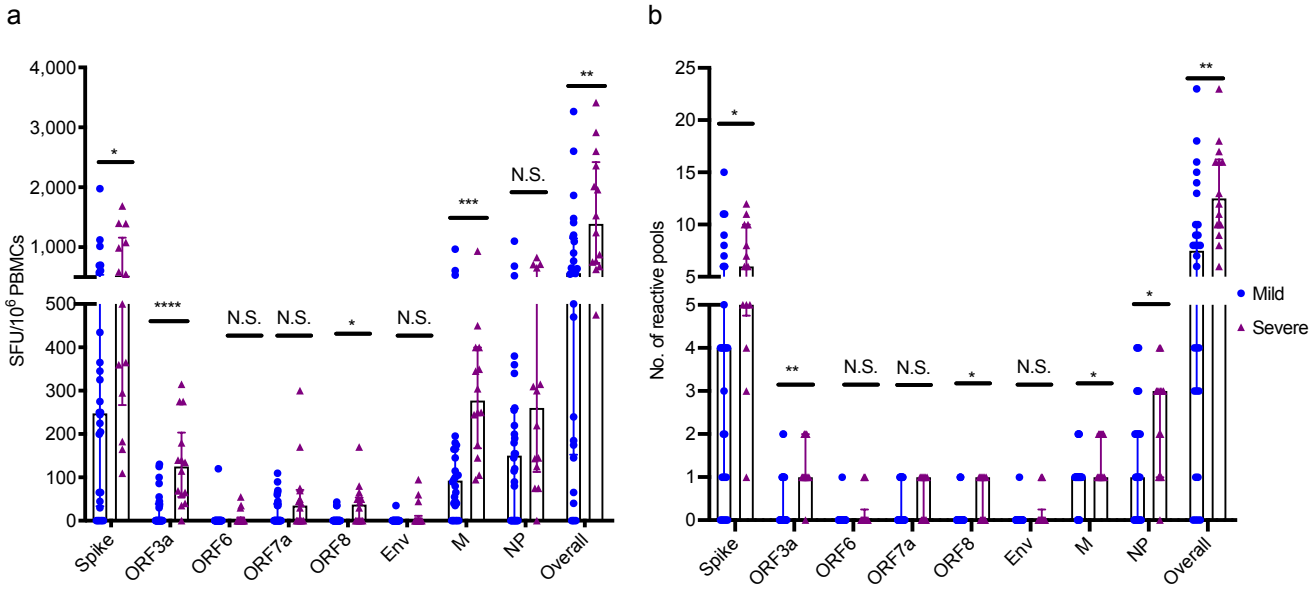
a
b
SFU/10^6 PBMCs
No. of reactive pools
Mild
Severe
Spike
ORF3a
ORF6
ORF7a
ORF8
Env
M
NP
Overall
N.S.

Figure 3

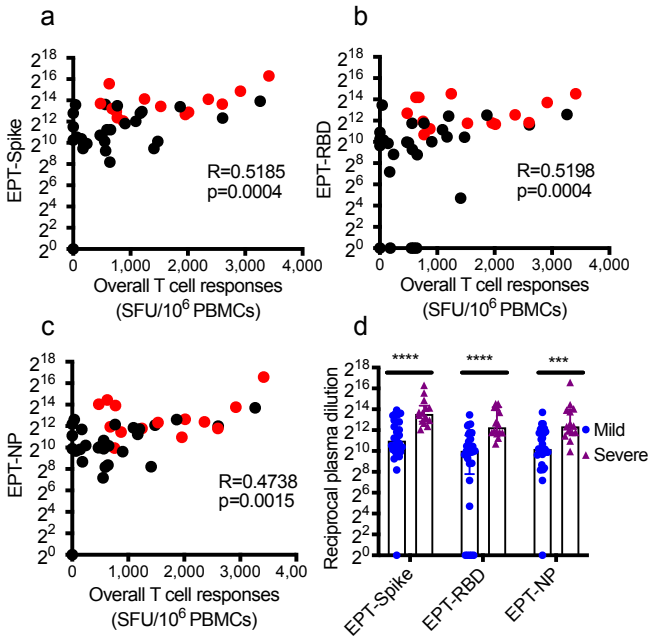
a
b
c
d
EPT-Spike
EPT-RBD
EPT-NP
R=0.5185
p=0.0004
R=0.5198
p=0.0004
R=0.4738
p=0.0015
Overall T cell responses
(SFU/10^6 PBMCs)
Reciprocal plasma dilution
****
****
***
Mild
Severe

Figure 4

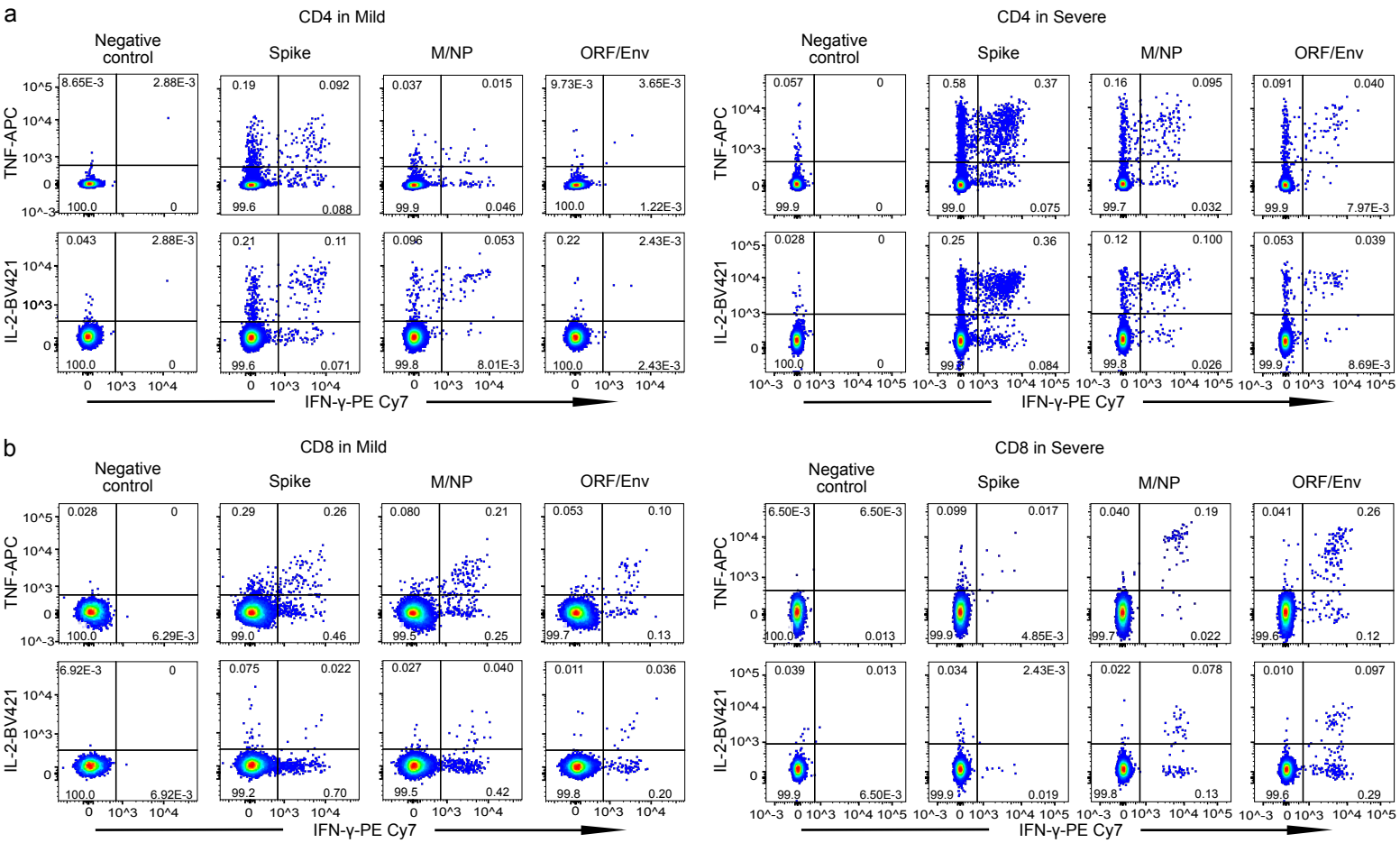
a
CD4 in Mild
CD4 in Severe
Negative control
Spike
M/NP
ORF/Env
TNF-APC
IL-2-BV421
IFN-γ-PE Cy7
b
CD8 in Mild
CD8 in Severe

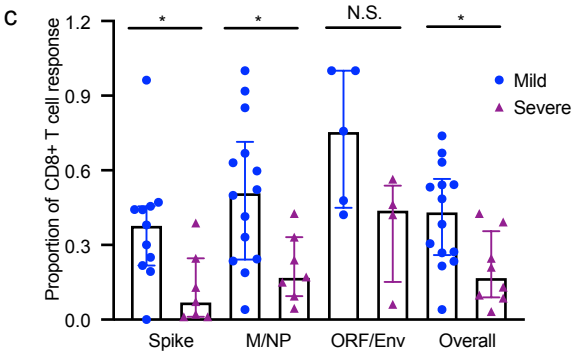
c
Proportion of CD8+ T cell response
Mild
Severe
N.S.
Spike
M/NP
ORF/Env
Overall

Figure 5

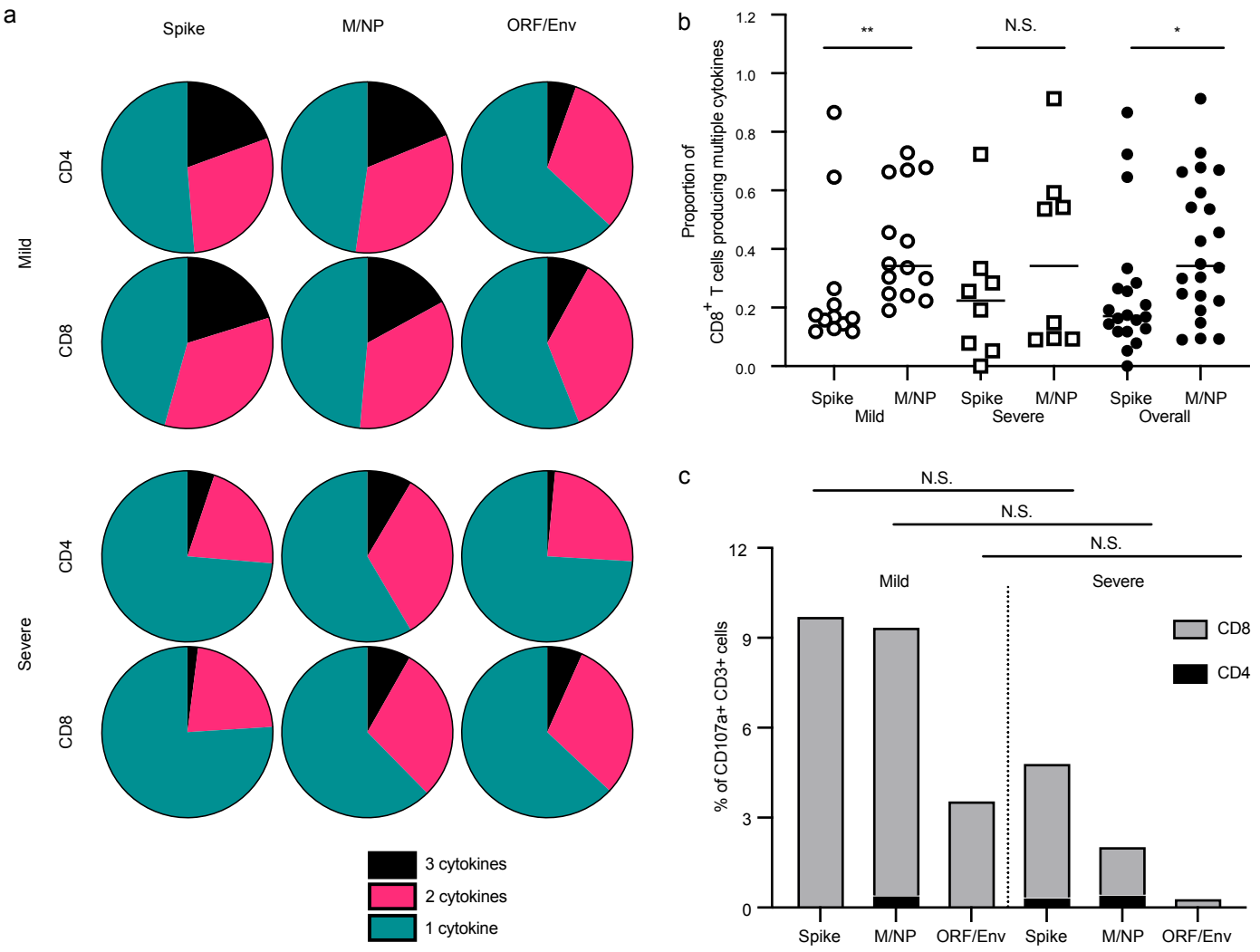
a
Spike
M/NP
ORF/Env
Mild
Severe
CD4
CD8
3 cytokines
2 cytokines
1 cytokine
b
Proportion of CD8+ T cells producing multiple cytokines
1.2
1.0
0.8
0.6
0.4
0.2
0.0
**
N.S.
*
Spike
M/NP
Mild
Severe
Overall
c
N.S.
N.S.
N.S.
% of CD107a+ CD3+ cells
12
9
6
3
0
CD8
CD4
ORF/Env

Figure 6

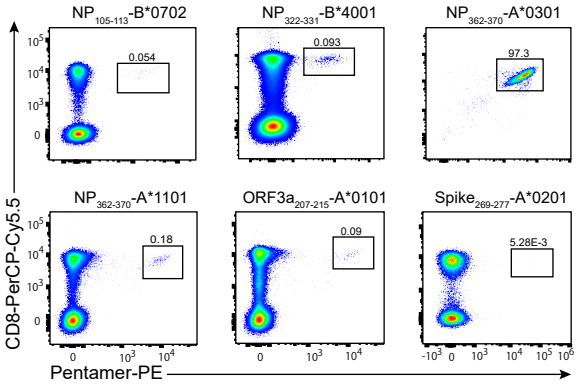
NP105-113-B*0702
NP322-331-B*4001
NP362-370-A*0301
NP362-370-A*1101
ORF3a207-215-A*0101
Spike269-277-A*0201
0.054
0.093
97.3
0.18
0.09
5.28E-3
CD8-PerCP-Cy5.5
Pentamer-PE

Figure 7

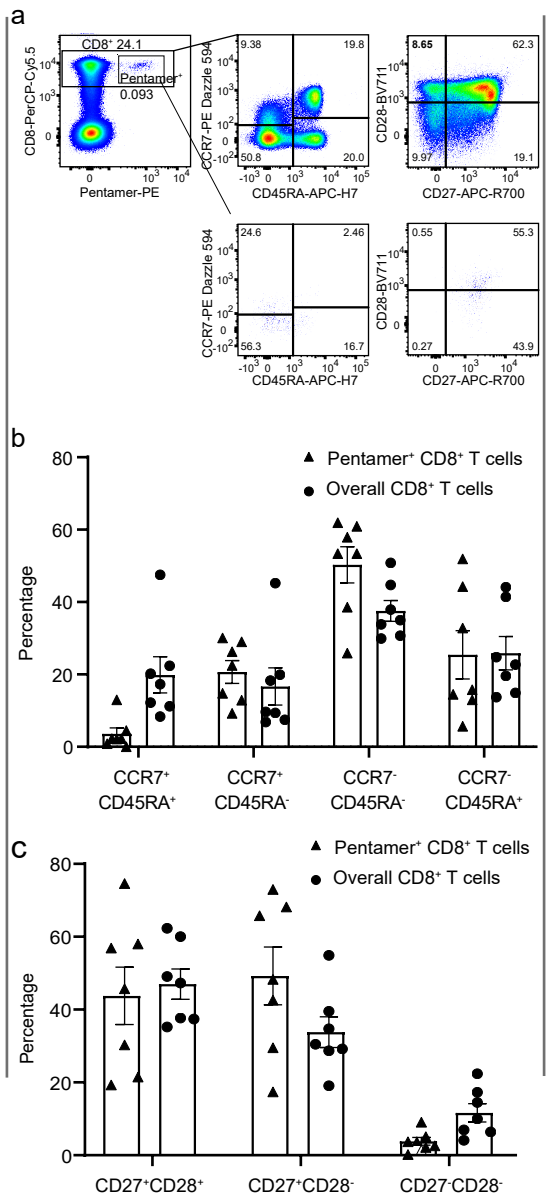
a
CD8+ 24.1
Pentamer+
0.093
CD8-PerCP-Cy5.5
Pentamer-PE
CCR7-PE Dazzle 594
CD45RA-APC-H7
9.38
19.8
50.8
20.0
CD28-BV711
CD27-APC-R700
8.65
62.3
9.97
19.1
24.6
2.46
56.3
16.7
0.55
55.3
0.27
43.9
b
Pentamer+ CD8+ T cells
Overall CD8+ T cells
Percentage
CCR7+ CD45RA+
CCR7+ CD45RA-
CCR7- CD45RA-
CCR7- CD45RA+
c
Pentamer+ CD8+ T cells
Overall CD8+ T cells
Percentage
CD27+CD28+
CD27+CD28-
CD27-CD28-

**Supplementary Fig. 1: Participant characteristics.** a) distribution of age, gender and days post symptom when sampling of the unexposed healthy controls and SSARS-CoV-2 infected patients studied. b) and c) Comparison of age (p=0.3465) and days post symptom (p=0.4075) when sampling between the patient groups with mild symptoms and severe symptoms. The unpaired t test with Welch's correction and Mann-Whitney test were used for data analysis of b) and c), respectively. Two tailed p value was calculated.

**a**

| | Unexposed (N=19) | Mild Disease (n=28,1 asymptomatic) | Severe Disease (n=14, 1 critical) |
|---|---|---|---|
| Age, y, median (IQR) | 46.0(31.0-53.0) | 53.8(47.6-60.9) | 60.6(44.9-74.1) |
| Male sex | 8(53.33) | 17(60.71) | 9(64.28) |
| Days post symptom, median (IQR) | NA | 42.5(40.2-55.7) | 41.5(40.0-47.5) |

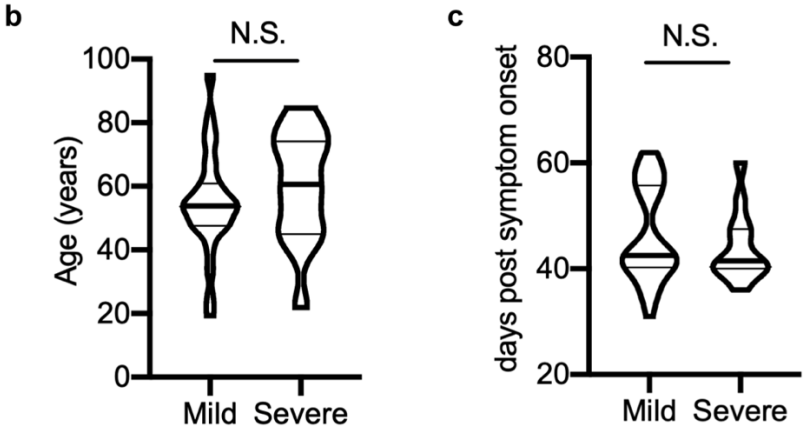


**Supplementary Fig. 2: No correlation between overall T cell response of each individual and the days post symptom when blood specimen was taken.** n=42. Black and red dots represent patients with history of mild symptoms and severe symptoms, respectively. Spearman's rank correlation coefficient was used for the correlation analysis, two tailed p value was calculated.

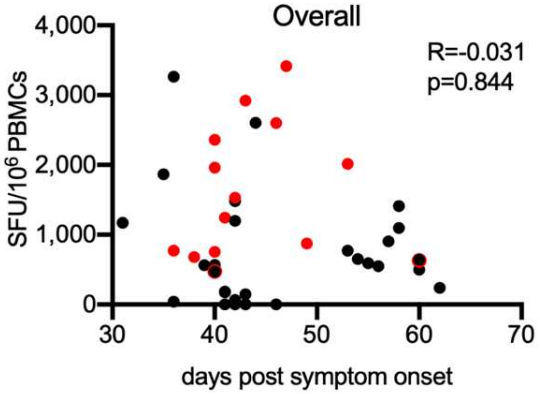

**Supplementary Fig. 3: Magnitude of T cell responses of unexposed healthy individuals against SARS-CoV-2 antigens.** a) An example of IFN-γ ELISpot plate from three healthy individuals without SARS-CoV-2 infection. Each individual has been tested with four spike pools (Pool 1-4, Pool 5-8, Pool 9-12 and Pool-13-16), 13 first dimension of non-spike pools and nine dominant individual peptides containing epitopes, along with six control wells including: negative controls with no peptide and peptide pools of irrelevant antigens derived from HIV Gag protein; positive controls with PHA and three pools of known $CD8^+$ T cell epitopes of human influenza, CMV and EBV viruses (namely FEC controls). b) Magnitude of T cell responses of unexposed healthy individuals against SARS-CoV-2 antigens and control antigens. n=16. Data are presented as median with interquartile range.

**a**

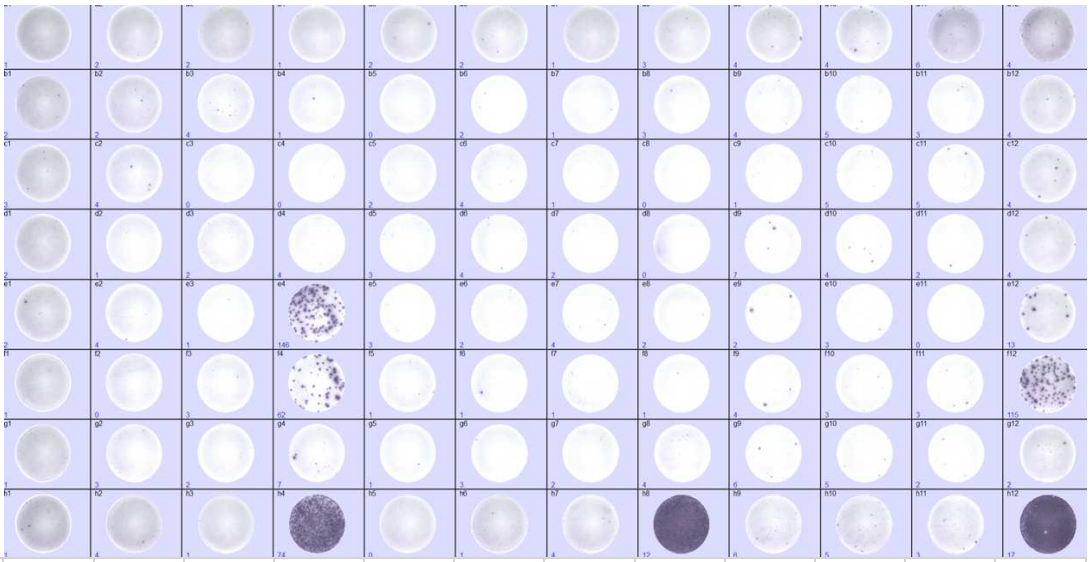

| | 1 | 2 | 3 | 4 | 5 | 6 | 7 | 8 | 9 | 10 | 11 | 12 |
|---|---|---|---|---|---|---|---|---|---|---|---|---|
| A | Spike-Pool1-4 | Pool-O-5 | Pool-O-13 | ORF7a-2 | Spike-Pool1-4 | Pool-O-5 | Pool-O-13 | ORF7a-2 | Spike-Pool1-4 | Pool-O-5 | Pool-O-13 | ORF7a-2 |
| B | Spike-Pool5-8 | Pool-O-6 | S-34 | OFR3-27 | Spike-Pool5-8 | Pool-O-6 | S-34 | OFR3-27 | Spike-Pool5-8 | Pool-O-6 | S-34 | OFR3-27 |
| C | Spike-Pool9-12 | Pool-O-7 | S-151 | RPMI NEG | Spike-Pool9-12 | Pool-O-7 | S-151 | RPMI NEG | Spike-Pool9-12 | Pool-O-7 | S-151 | RPMI NEG |
| D | Spike-Pool13-16 | Pool-O-8 | M-24 | HIV | Spike-Pool13-16 | Pool-O-8 | M-24 | HIV | Spike-Pool13-16 | Pool-O-8 | M-24 | HIV |
| E | Pool-O-1 | Pool-O-9 | NP-16 | FLU | Pool-O-1 | Pool-O-9 | NP-16 | FLU | Pool-O-1 | Pool-O-9 | NP-16 | FLU |
| F | Pool-O-2 | Pool-O-10 | S-174 | CMV | Pool-O-2 | Pool-O-10 | S-174 | CMV | Pool-O-2 | Pool-O-10 | S-174 | CMV |
| G | Pool-O-3 | Pool-O-11 | M-20 | EBV | Pool-O-3 | Pool-O-11 | M-20 | EBV | Pool-O-3 | Pool-O-11 | M-20 | EBV |
| H | Pool-O-4 | Pool-O-12 | NP-48 | PHA | Pool-O-4 | Pool-O-12 | NP-48 | PHA | Pool-O-4 | Pool-O-12 | NP-48 | PHA |

**b**

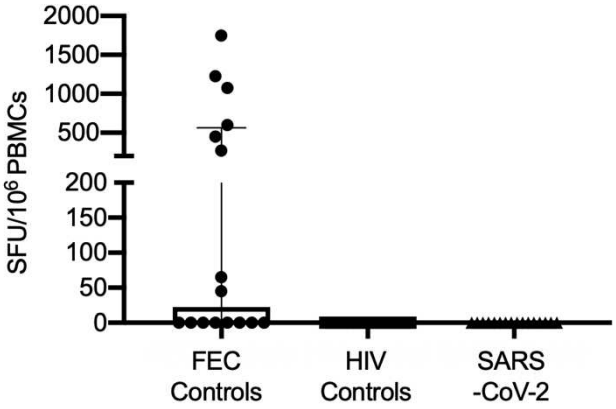

**Supplementary Fig. 4: Correlation between SARS-CoV-2 antigen-specific T cell responses and SARS-CoV-2 antigen-specific antibody responses.** a), b) and c) Correlation of Spike-, RBD-, and NP-specific antibody responses to corresponding antigen-specific T cell responses. d) Correlation between NP-specific antibody response and Spike-specific T cell response. n=42. Black and red dots represent patients with history of mild symptoms and severe symptoms, respectively. Spearman's rank correlation coefficient was used for the correlation analysis, two tailed p value was calculated.

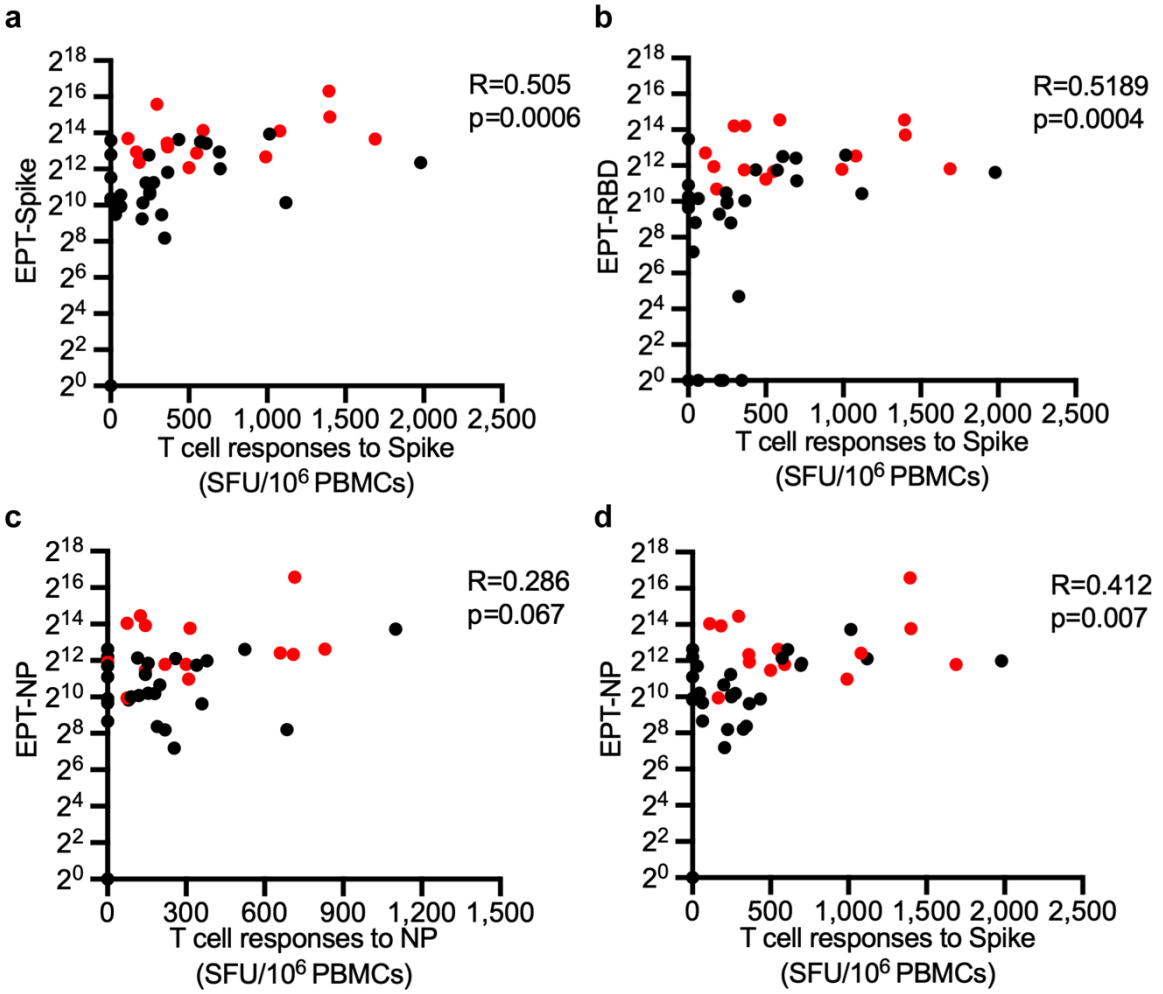

**Supplementary Fig. 5: Gating strategy of flow cytometry analysis.** a) Gating for $CD4^+/CD8^+$ T cells. Cells were gated on single cell by a forward side scatter gate, followed by CD3/ CD4/CD8 gating excluding dead cells, $CD14^+$, $CD19^+$, and $CD16^+$ cells. This gating strategy was used for Fig. 4-7 and Supplementary Fig. 6. b) Gating for IFNγ+/-, TNF$\alpha^{+/-}$, IL-$2^{+/-}$, and $CD107a^{+/-}$ population were based on corresponding negative controls. This gating strategy was used for Fig. 4-5.

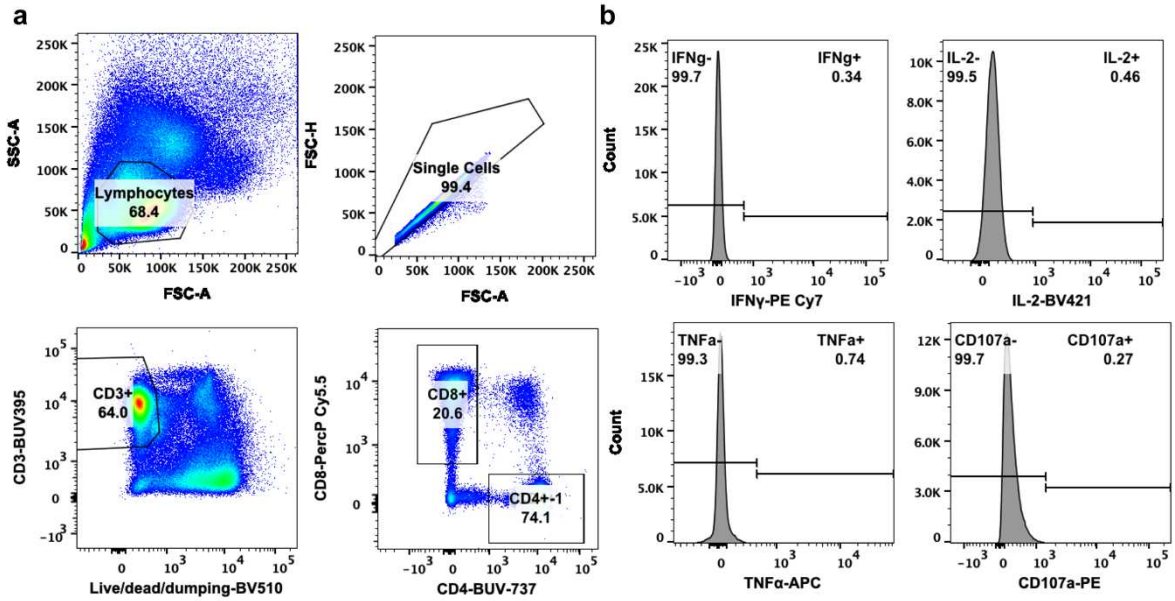


**Supplementary Fig. 6: Comparison of Cytokine production of T cells between the patients with different disease severity and T cells targeting different viral proteins.** a) No significant difference in the percentage of CD4+ and CD8+ T cells producing IFN-γ and/or TNFα, and/or IL-2 targeting each viral antigen between mild cases (n=14) and severe cases (n=8). Data are shown in value of median. b) No significant difference in proportion of multifunctional CD4+ T cells targeting spike protein (Mild group, n=12; Severe group, n=8) and M/NP protein (Mild group, n=14; Severe group, n=8). Mann-Whitney test was used for the analysis. Two-tailed p value was calculated. N.S. P>0.05

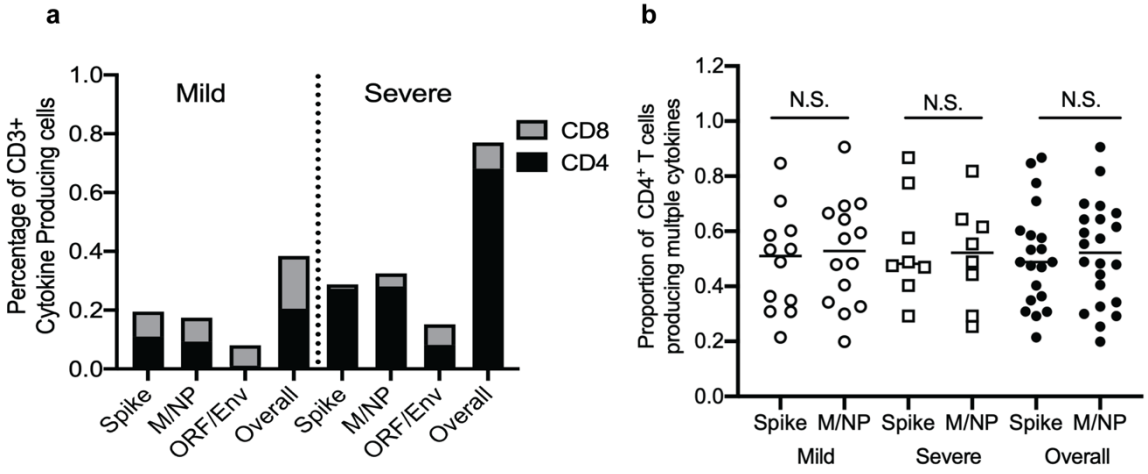

**Supplementary Fig. 7: Confirmation of dominant T cell responses with cultured short-term T cell lines.** Patient C-COV19-028 showed a CD4 T cell response to peptide S-34 and CD8 T cell response to peptide NP-51. Patient C-COV-19-038 showed CD4 T cell response to three dominant peptides: S-151 (weak), S-174, M24 and a CD8 T cell response to NP-16. Patient C-COV-19-039 showed CD4 T cell response to peptide S-E-19, whereas donor C-COV19-031 had a CD4 T cell response targeting peptide M-20. PBMCs were stimulated with corresponding peptide pools corresponding to the ex vivo ELISpot results and then cultured for 10 days. Cytokine production of the cell lines was then examined by ICS upon the stimulation with single peptides. Cells were gated on the live/singlet/ CD3+ Lymphocyte population.

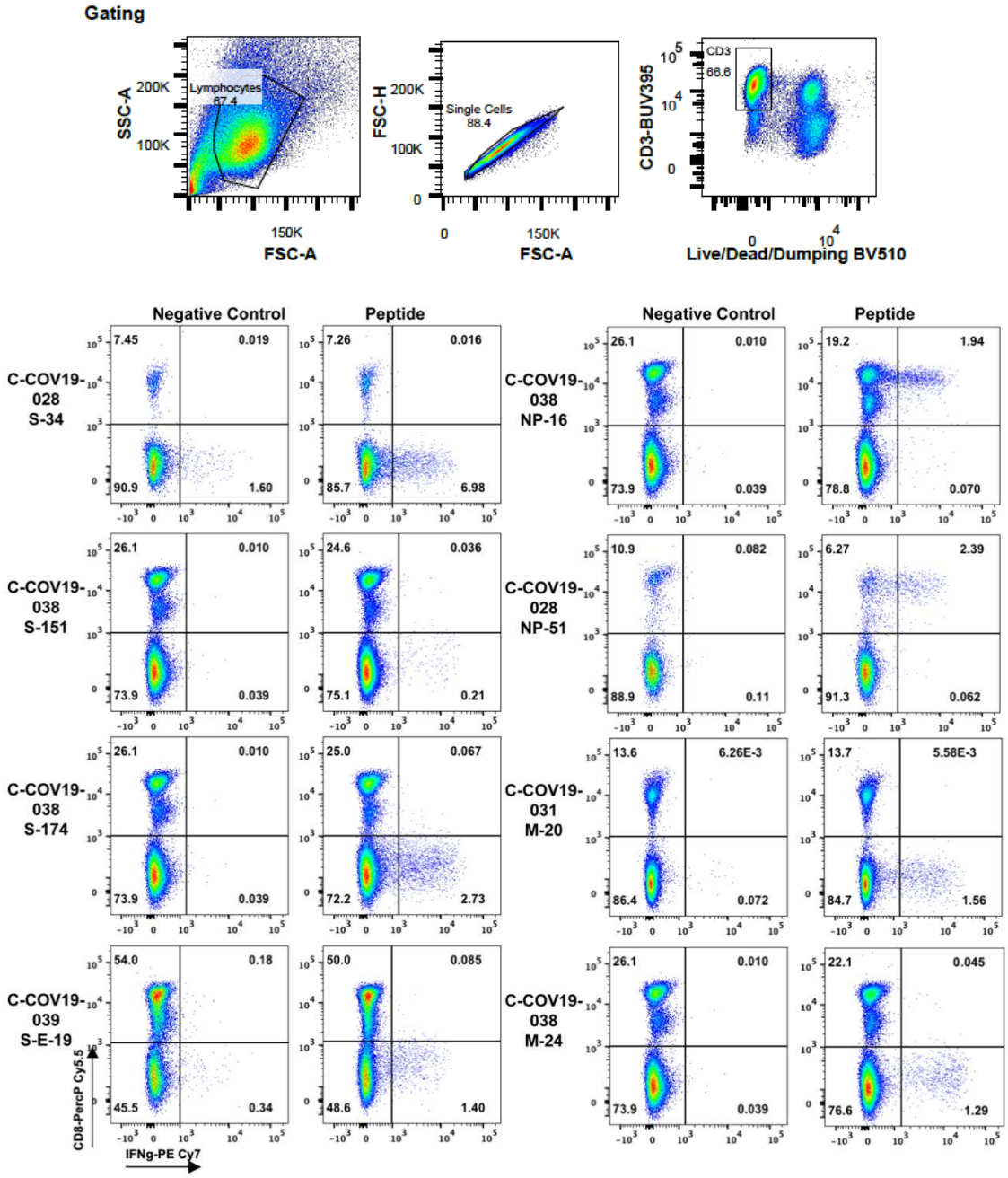

**Supplementary Table 1: Two-dimensional peptide Matrix pools**.

a: Spike protein: 253 peptides in total 32 pools including 16 pools in 1st dimension and 16 pools in 2nd dimension

| | Pool-17 | Pool-18 | Pool-19 | Pool-20 | Pool-21 | Pool-22 | Pool-23 | Pool-24 | Pool-25 | Pool-26 | Pool-27 | Pool-28 | Pool-29 | Pool-30 | Pool-31 | Pool-32 |
|---|---|---|---|---|---|---|---|---|---|---|---|---|---|---|---|---|
| **Pool 1** | S-1 | S-2 | S-3 | S-4 | S-5 | S-6 | S-7 | S-8 | S-9 | S-10 | S-11 | S-12 | S-13 | S-14 | S-15 | S-16 |
| **Pool 2** | S-17 | S-18 | S-19 | S-20 | S-21 | S-22 | S-23 | S-24 | S-25 | S-26 | S-27 | S-28 | S-29 | S-30 | S-31 | S-32 |
| **Pool 3** | S-33 | S-34 | S-35 | S-36 | S-37 | S-38 | S-39 | S-40 | S-41 | S-42 | S-43 | S-44 | S-45 | S-46 | S-47 | S-48 |
| **Pool 4** | S-49 | S-50 | S-51 | S-52 | S-53 | S-54 | S-55 | S-56 | S-57 | S-58 | S-59 | S-60 | S-61 | S-62 | S-63 | S-64 |
| **Pool 5** | S-65 | S-66 | S-67 | S-68 | S-69 | S-70 | S-71 | S-72 | S-73 | S-74 | S-75 | S-76 | S-77 | S-78 | S-79 | S-80 |
| **Pool 6** | S-81 | S-82 | S-83 | S-84 | S-85 | S-86 | S-87 | S-88 | S-89 | S-90 | S-91 | S-92 | S-93 | S-94 | S-95 | S-96 |
| **Pool 7** | S-97 | S-98 | S-99 | S-100 | S-101 | S-102 | S-103 | S-104 | S-105 | S-106 | S-107 | S-108 | S-109 | S-110 | S-111 | S-112 |
| **Pool 8** | S-113 | S-114 | S-115 | S-116 | S-117 | S-118 | S-119 | S-120 | S-121 | S-122 | S-123 | S-124 | S-125 | S-126 | S-127 | S-128 |
| **Pool 9** | S-129 | S-130 | S-131 | S-132 | S-133 | S-134 | S-135 | S-136 | S-137 | S-138 | S-139 | S-140 | S-141 | S-142 | S-143 | S-144 |
| **Pool 10** | S-145 | S-146 | S-147 | S-148 | S-149 | S-150 | S-151 | S-152 | S-153 | S-154 | S-155 | S-156 | S-157 | S-158 | S-159 | S-160 |
| **Pool 11** | S-161 | S-162 | S-163 | S-164 | S-165 | S-166 | S-167 | S-168 | S-169 | S-170 | S-171 | S-172 | S-173 | S-174 | S-175 | S-176 |
| **Pool 12** | S-177 | S-178 | S-179 | S-180 | S-181 | S-182 | S-183 | S-184 | S-185 | S-186 | S-187 | S-188 | S-189 | S-190 | S-191 | S-192 |
| **Pool 13** | S-193 | S-194 | S-195 | S-196 | S-197 | S-198 | S-199 | S-200 | S-201 | S-202 | S-203 | S-204 | S-205 | S-206 | S-207 | S-208 |
| **Pool 14** | S-209 | S-210 | S-211 | S-212 | S-213 | S-214 | S-215 | S-216 | S-217 | S-218 | S-219 | S-220 | S-221 | S-222 | S-223 | S-224 |
| **Pool 15** | S-225 | S-226 | S-227 | S-228 | S-229 | S-230 | S-231 | S-232 | S-233 | S-234 | S-235 | S-236 | S-237 | S-238 | S-239 | S-240 |
| **Pool 16** | S-241 | S-242 | S-243 | S-244 | S-245 | S-246 | S-247 | S-248 | S-249 | S-250 | S-251 | S-252 | S-253 | | | |

b: Non-spike proteins: total 29 pools, 13 pools in 1st dimension including ORF3a (35 peptides in 3 pools), ORF6 (7 peptides in 1 pool), ORF7a(15 peptides in 1 pool), ORF8(16 peptides in 1 pool), Envelope(9 peptides in 1 pool), Membrane Protein(29 peptides in 2 pools) and Nucleoprotein( 59 peptides in 4 pools).

| | Pool-O-14 | Pool-O-15 | Pool-O-16 | Pool-O-17 | Pool-O-18 | Pool-O-19 | Pool-O-20 | Pool-O-21 | Pool-O-22 | Pool-O-23 | Pool-O-24 | Pool-O-25 | Pool-O-26 | Pool-O-27 | Pool-O-28 | Pool-O-29 |
|---|---|---|---|---|---|---|---|---|---|---|---|---|---|---|---|---|
| **Pool-O-1** | ORF3a-1 | ORF3a-2 | ORF3a-3 | ORF3a-4 | ORF3a-5 | ORF3a-6 | ORF3a-7 | ORF3a-8 | ORF3a-9 | ORF3a-10 | ORF3a-11 | ORF3a-12 | ORF3a-13 | ORF3a-14 | ORF3a-15 | ORF3a-16 |
| **Pool-O-2** | ORF3a-17 | ORF3a-18 | ORF3a-19 | ORF3a-20 | ORF3a-21 | ORF3a-22 | ORF3a-23 | ORF3a-24 | ORF3a-25 | ORF3a-26 | ORF3a-27 | ORF3a-28 | ORF3a-29 | ORF3a-30 | ORF3a-31 | ORF3a-32 |
| **Pool-O-3** | ORF3a-33 | ORF3a-34 | ORF3a-35 | | | | | | | | | | | | | |
| **Pool-O-4** | ORF6-1 | ORF6-2 | ORF6-3 | ORF6-4 | ORF6-5 | ORF6-6 | ORF6-7 | | | | | | | | | |
| **Pool-O-5** | ORF7a-1 | ORF7a-2 | ORF7a-3 | ORF7a-4 | ORF7a-5 | ORF7a-6 | ORF7a-7 | ORF7a-8 | ORF7a-9 | ORF7a-10 | ORF7a-11 | ORF7a-12 | ORF7a-13 | ORF7a-14 | ORF7a-15 | |
| **Pool-O-6** | ORF8-1 | ORF8-2 | ORF8-3 | ORF8-4 | ORF8-5 | ORF8-6 | ORF8-7 | ORF8-8 | ORF8-9 | ORF8-10 | ORF8-11 | ORF8-12 | ORF8-13 | ORF8-14 | ORF8-15 | ORF8-16 |
| **Pool-O-7** | Env-1 | Env-2 | Env-3 | Env-4 | Env-5 | Env-6 | Env-7 | Env-8 | Env-9 | | | | | | | |
| **Pool-O-8** | M-1 | M-2 | M-3 | M-4 | M-5 | M-6 | M-7 | M-8 | M-9 | M-10 | M-11 | M-12 | M-13 | M-14 | M-15 | M-16 |
| **Pool-O-9** | M-17 | M-18 | M-19 | M-20 | M-21 | M-22 | M-23 | M-24 | M-25 | M-26 | M-27 | M-28 | | | | |
| **Pool-O-10** | NP-1 | NP-2 | NP-3 | NP-4 | NP-5 | NP-6 | NP-7 | NP-8 | NP-9 | NP-10 | NP-11 | NP-12 | NP-13 | NP-14 | NP-15 | NP-16 |
| **Pool-O-11** | NP-17 | NP-18 | NP-19 | NP-20 | NP-21 | NP-22 | NP-23 | NP-24 | NP-25 | NP-26 | NP-27 | NP-28 | NP-29 | NP-30 | NP-31 | NP-32 |
| **Pool-O-12** | NP-33 | NP-34 | NP-35 | NP-36 | NP-37 | NP-38 | NP-39 | NP-40 | NP-41 | NP-42 | NP-43 | NP-44 | NP-45 | NP-46 | NP-47 | NP-48 |
| **Pool-O-13** | NP-49 | NP-50 | NP-51 | NP-52 | NP-53 | NP-54 | NP-55 | NP-56 | NP-57 | NP-58 | | | | | | |

**Supplementary Table 2: HLA class I typing of CD8$^+$ epitope peptides in subjects with confirmed responses.** Each patient listed made a CD8 T cell response to the peptides shown. Optimal epitopes and the corresponding HLA-restriction were predicted by IEDB analysis tool (http://tools.iedb.org/mhci). Red highlights are the predicted optimal epitope sequences.

| Protein | Peptide ID | Peptide sequence | Predicted HLA Restriction | Patients | HLA A1 | A2 | B1 | B2 | Cw1 | Cw2 |
|---|---|---|---|---|---|---|---|---|---|---|
| NP | NP-1 | MSDNGPQNQRNAPRITF | B*2705/06 | C-COV19-044 | 02:07 | 11:01 | 27:06 | 40:01 | 03:04 | 07:02 |
| | NP-2 | NQRNAPRITFGGPSDSTG | | C-COV19-047 | 24:02 | 24:02 | 27:05 | 27:05 | 01:02 | 02:02 |
| | | | | C-COV19-025 | 02:01 | 24:02 | 27:05 | 44:02 | 02:02 | 05:01/03 |
| | NP-16 | LSPRWYFYYLGTGPEAGL | B*0702 | C-COV19-001 | 02:01 | 23:01 | 07:02 | 49:01 | 07:01 | 07:02 |
| | | LSPRWYFYYLGTGPEAGL | A*0201 | C-COV19-002 | 03:01 | 68:02 | 07:02 | 49:01 | 06:02 | 07:02 |
| | | LSPRWYFYYLGTGPEAGL | Cw*0702 | C-COV19-003 | 02:01 | 32:01 | 07:02 | 44:02 | 05:01/03 | 07:02 |
| | | | | C-COV19-004 | 02:01 | 02:01 | 07:02 | 40:01 | 03:04 | 07:02 |
| | | | | C-COV19-005 | 01:01/04N | 02:01 | 07:02 | 40:01 | 01:02 | 07:02 |
| | | | | C-COV19-006 | 01:01/04N | 29:02 | 07:02 | 45:01 | 07:01 | 07:02 |
| | | | | C-COV19-007 | 01:01/04N | 01:01/04N | 07:02 | 07:02 | 07:02 | 07:02 |
| | | | | C-COV19-035 | 11:01 | 11:01 | 07:02 | 07:05/06 | 03:04 | 07:02 |
| | | | | C-COV19-036 | 01:01/04N | 03:01 | 07:02 | 52:01 | 07:02 | 12:02 |
| | | | | C-COV19-038 | 02:01 | 24:02 | 07:02 | 51:01 | 04:01 | 07:02 |
| | | | | C-COV19-045 | 01:01/04N | 02:01 | 07:02 | 45:01 | 06:02 | 07:02 |
| | | | | C-COV19-046 | 02:01 | 03:01 | 07:02 | 44:02 | 05:01/03 | 07:02 |
| | NP-E-3 | MEVTPSGTWL | B*4001 | C-COV19-021 | 02:01 | 31:01 | 40:01 | 40:01 | 03:04 | 03:04 |
| | | | | C-COV19-044 | 02:07 | 11:01 | 27:06 | 40:01 | 03:04 | 07:02 |
| | NP-51 | LLNKHIDAYKTFPPTEPK | A*0301 | C-COV19-028 | 02:01 | 03:01 | 15:01 | 44:02 | 03:03 | 07:04/11 |
| | | | | C-COV19-036 | 01:01/04N | 03:01 | 07:02 | 52:01 | 07:02 | 12:02 |
| | NP-51 | LLNKHIDAYKTFPPTEPK | A*1101 | C-COV19-035 | 11:01 | 11:01 | 07:02 | 07:05/06 | 03:04 | 07:02 |
| ORF | ORF3a-27 | KDCVVLHSYFTSDYYQLY | A*0101 | C-COV19-022 | 01:01/04N | 01:01/04N | 08:01 | 08:01 | 07:01 | 07:02 |
| | ORF3a-28 | YFTSDYYQLYSTQLSTDTGV | | C-COV19-036 | 01:01/04N | 03:01 | 07:02 | 52:01 | 07:02 | 12:02 |
| | | | | C-COV19-037 | 01:01/04N | 26:01 | 08:01 | 38:01 | 07:01 | 12:03 |
| | | | | C-COV19-040 | 01:04N | 03:01 | 27:05 | 57:01 | 01:02 | 06:02 |
| Spike | S-34 | CTFEYVSQPFLMDLE | Cw*0702 | C-COV19-035 | 11:01 | 11:01 | 07:02 | 07:05/06 | 03:04 | 07:02 |
| | S-106 | GPKKSTNLVKNKCVN | A*3101 | C-COV19-021 | 02:01 | 31:01 | 40:01 | 40:01 | 03:04 | 03:04 |

**Supplementary Table 3: Known SARS epitopes with identical sequences to SARS-CoV-2 , and Tetramers/Pentamers.** Red highlights the epitope responses detected in the patients who had recovered from COVID-19, whether by tetramer/pentamer staining or ELISpot assay.

| Peptide ID | Epitope | Protein | MHC allele | Tetramer/Pentamer |
|---|---|---|---|---|
| **N-E-01** | ILLNKHID | NP | HLA-A*02:01 | Y |
| **N-E-02** | AFFGMSRIGMEVTPSGTW | NP | NA | |
| **N-E-03** | MEVTPSGTWL | NP | HLA-B*40:01 I | Y |
| **N-E-04** | GMSRIGMEV | NP | HLA-A*02:01 I | Y |
| **N-E-05** | ILLNKHIDA | NP | HLA-A*02:01 I | Y |
| **N-E-06** | ALNTPKDHI | NP | HLA-A*02:01 I | Y |
| **N-E-07** | IRQGTDYKHWPQIAQFA | NP | NA | |
| **N-E-08** | KHWPQIAQFAPSASAFF | NP | NA | |
| **N-E-09** | LALLLLDRL | NP | HLA-A*02:01 I | Y |
| **N-E-10** | LLLDRLNQL | NP | HLA-A*02:01 I | Y |
| **N-E-11** | LLNKHIDAYKTFPPTEPK | NP | NA | |
| **N-E-12** | LQLPQGTTL | NP | HLA-A*02:01 I | Y |
| **N-E-13** | AQFAPSASAFFGMSR | NP | NA | |
| **N-E-14** | AQFAPSASAFFGMSRIGM | NP | NA | |
| **N-E-15** | RRPQGLPNNTASWFT | NP | NA I | |
| **N-E-16** | YKTFPPTEPKKDKKKK | NP | NA | |
| **S-E-17** | GAALQIPFAMQMAYRF | Spike | HLA-DRA*01:01,HLA-DRB1*07:01 | Y |
| **S-E-18** | MAYRFNGIGVTQNVLY | Spike | HLA-DRB1*04:01 | Y |
| **S-E-19** | QLIRAAEIRASANLAATK | Spike | HLA-DRB1*04:01 | Y |
| **S-E-20** | FIAGLIAIV | Spike | HLA-A*02:01 | Y |
| **S-E-21** | ALNTLVKQL | Spike | HLA-A*02:01 I | Y |
| **S-E-22** | LITGRLQSL | Spike | HLA-A2 I | Y |
| **S-E-23** | NLNESLIDL | Spike | HLA-A*02:01 I | Y |
| **S-E-24** | QALNTLVKQLSSNFGAI | Spike | HLA-DRB1*04:01 | Y |
| **S-E-25** | RLNEVAKNL | Spike | HLA-A*02:01 I | Y |
| **S-E-26** | VLNDILSRL | Spike | HLA-A*02:01 I | Y |
| **S-E-27** | VVFLHVTYV | Spike | HLA-A*02:01 I | Y |

**Supplementary Table 4:**

**Oxford Immunology Network Covid-19 response: T cell Immunity Team**

**Team leader:** Graham Ogg,

Barbara Kronsteiner, Anthony Brown, Emily Adland, Patpong Rongkard, Anna Csala, Helen Brown, Nicola Robinson, Panagiota Zacharopoulou, Vinicius Adriano, Prabhjeet Phalora, Oliver Sampson, Carl-Philipp Hackstein, Nicholas Lim, Matt Edmans, Senthil Chinnakannan, Rachael Brown, Ali Amini, Mathew Jones, Mohammad Ali, Timothy Donnison, Matt Pace, Ane Ogbe, Donal Skelly, Lizzie Stafford, Helen Fletcher, Lian Lee, Prathiba Kurupati, Rachel Etherington, Nicholas Provine, Hashem Koohy, Chloe Hyun-Jung Lee, Yanchun Peng, Guihai Liu, Xuan Yao, Zixi Yin, Danning Dong, Mariolina Salio, Giorgio Napolitani, Susanna Dunachie, Eleanor Barnes, John Frater, Georgina Kerr, Philip Goulder, Paul Klenerman, Andrew McMichael, Tao Dong.

**Supplementary Table 5: ISARIC 4C Investigators**

**Consortium Lead Investigator:** J Kenneth Baillie,
**Chief Investigator:** Malcolm G Semple
**Co-Lead Investigator:** Peter JM Openshaw.
**ISARIC Clinical Coordinator**: Gail Carson.
**Co-Investigators:** Beatrice Alex, Benjamin Bach, Wendy S Barclay, Debby Bogaert, Meera Chand, Graham S Cooke, Annemarie B Docherty, Jake Dunning, Ana da Silva Filipe, Tom Fletcher, Christopher A Green, Ewen M Harrison, Julian A Hiscox, Antonia Ying Wai Ho, Peter W Horby, Samreen Ijaz, Saye Khoo, Paul Klenerman, Andrew Law, Wei Shen Lim, Alexander, J Mentzer, Laura Merson, Alison M Meynert, Mahdad Noursadeghi, Shona C Moore, Massimo Palmarini, William A Paxton, Georgios Pollakis, Nicholas Price, Andrew Rambaut, David L Robertson, Clark D Russell, Vanessa Sancho-Shimizu, Janet T Scott, Louise Sigfrid, Tom Solomon, Shiranee Sriskandan, David I Stuart, Charlotte Summers, Richard S Tedder, Emma C Thomson, Ryan S Thwaites, Lance Turtle, Maria Zambon. Project Managers Hayley Hardwick, Chloe Donohue, Jane Ewins, Wilna Oosthuyzen, Fiona Griffiths. Data Analysts: Lisa Norman, Riinu Pius, Tom M Drake, Cameron J Fairfield, Stephen Knight, Kenneth A Mclean, Derek Murphy, Catherine A Shaw. Data and Information System Manager: Jo Dalton, Michelle Girvan, Egle Saviciute, Stephanie Roberts Janet Harrison, Laura Marsh, Marie Connor. Data integration and presentation: Gary Leeming, Andrew Law, Ross Hendry. Material Management: William Greenhalf, Victoria Shaw, Sarah McDonald. Outbreak Laboratory Volunteers: Katie A. Ahmed, Jane A Armstrong, Milton Ashworth, Innocent G Asiimwe, Siddharth Bakshi, Samantha L Barlow, Laura Booth, Benjamin Brennan, Katie Bullock, Benjamin WA Catterall, Jordan J Clark, Emily A Clarke, Sarah Cole, Louise Cooper, Helen Cox, Christopher Davis, Oslem Dincarslan, Chris Dunn, Philip Dyer, Angela Elliott, Anthony Evans, Lewis WS Fisher, Terry Foster, Isabel Garcia-Dorival, Willliam Greenhalf, Philip Gunning, Catherine Hartley, Antonia Ho, Rebecca L Jensen, Christopher B Jones, Trevor R Jones, Shadia Khandaker, Katharine King, Robyn T. Kiy, Chrysa Koukorava, Annette Lake, Suzannah Lant, Diane Latawiec, L Lavelle-Langham, Daniella Lefteri, Lauren Lett, Lucia A Livoti, Maria Mancini, Sarah McDonald, Laurence McEvoy, John McLauchlan, Soeren Metelmann, Nahida S Miah, Joanna Middleton, Joyce Mitchell, Shona C Moore, Ellen G Murphy, Rebekah Penrice-Randal, Jack Pilgrim, Tessa Prince, Will Reynolds, P. Matthew Ridley, Debby Sales, Victoria E Shaw, Rebecca K Shears, Benjamin Small, Krishanthi S Subramaniam, Agnieska Szemiel, Aislynn Taggart, Jolanta Tanianis, Jordan Thomas, Erwan Trochu, Libby van Tonder, Eve Wilcock, J. Eunice Zhang. Local Principal Investigators: Kayode Adeniji, Daniel Agranoff, Ken Agwuh, Dhiraj Ail, Ana Alegria, Brian Angus, Abdul Ashish, Dougal Atkinson, Shahedal Bari, Gavin Barlow, Stella Barnass, Nicholas Barrett, Christopher Bassford, David Baxter, Michael Beadsworth, Jolanta Bernatoniene, John Berridge , Nicola Best , Pieter Bothma, David Brealey, Robin Brittain-Long, Naomi Bulteel, Tom Burden , Andrew Burtenshaw, Vikki Caruth, David

Chadwick, Duncan Chambler, Nigel Chee, Jenny Child, Srikanth Chukkambotla, Tom Clark, Paul Collini, Catherine Cosgrove, Jason Cupitt, Maria-Teresa Cutino-Moguel, Paul Dark, Chris Dawson, Samir Dervisevic, Phil Donnison, Sam Douthwaite, Ingrid DuRand, Ahilanadan Dushianthan, Tristan Dyer, Cariad Evans , Chi Eziefula, Chrisopher Fegan, Adam Finn, Duncan Fullerton, Sanjeev Garg, Sanjeev Garg, Atul Garg, Jo Godden, Arthur Goldsmith, Clive Graham, Elaine Hardy, Stuart Hartshorn, Daniel Harvey, Peter Havalda, Daniel B Hawcutt, Maria Hobrok, Luke Hodgson, Anita Holme, Anil Hormis, Michael Jacobs, Susan Jain, Paul Jennings, Agilan Kaliappan, Vidya Kasipandian, Stephen Kegg, Michael Kelsey, Jason Kendall, Caroline Kerrison, Ian Kerslake, Oliver Koch, Gouri Koduri, George Koshy , Shondipon Laha, Susan Larkin, Tamas Leiner, Patrick Lillie, James Limb, Vanessa Linnett, Jeff Little, Michael MacMahon, Emily MacNaughton, Ravish Mankregod, Huw Masson , Elijah Matovu, Katherine McCullough, Ruth McEwen , Manjula Meda, Gary Mills , Jane Minton, Mariyam Mirfenderesky, Kavya Mohandas, Quen Mok, James Moon, Elinoor Moore, Patrick Morgan, Craig Morris, Katherine Mortimore, Samuel Moses, Mbiye Mpenge, Rohinton Mulla, Michael Murphy, Megan Nagel, Thapas Nagarajan, Mark Nelson, Igor Otahal, Mark Pais, Selva Panchatsharam, Hassan Paraiso, Brij Patel, Justin Pepperell, Mark Peters, Mandeep Phull , Stefania Pintus, Jagtur Singh Pooni, Frank Post, David Price, Rachel Prout, Nikolas Rae, Henrik Reschreiter, Tim Reynolds, Neil Richardson, Mark Roberts, Devender Roberts, Alistair Rose, Guy Rousseau, Brendan Ryan, Taranprit Saluja, Aarti Shah, Prad Shanmuga, Anil Sharma, Anna Shawcross, Jeremy Sizer, Richard Smith, Catherine Snelson, Nick Spittle, Nikki Staines , Tom Stambach, Richard Stewart, Pradeep Subudhi, Tamas Szakmany, Kate Tatham, Jo Thomas, Chris Thompson, Robert Thompson, Ascanio Tridente, Darell Tupper - Carey, Mary Twagira, Andrew Ustianowski, Nick Vallotton, Lisa Vincent-Smith, Shico Visuvanathan , Alan Vuylsteke, Sam Waddy, Rachel Wake, Andrew Walden, Ingeborg Welters, Tony Whitehouse, Paul Whittaker, Ashley Whittington, Meme Wijesinghe, Martin Williams, Lawrence Wilson, Sarah Wilson, Stephen Winchester, Martin Wiselka, Adam Wolverson, Daniel G Wooton, Andrew Workman, Bryan Yates, Peter Young.